

Pavel A. Bakhvalov, Alexey P. Duben, Tatiana K. Kozubskaya and Pavel V. Rodionov

Extension of the EBR schemes to prismatic layers using the quasi-1D curvilinear reconstructions of variables

Computational Aerodynamics and Aeroacoustics Laboratory

Keldysh Institute of Applied Mathematics, Moscow



Compressible Navier–Stokes equations:

$$\frac{\partial \mathbf{Q}}{\partial t} + \nabla \cdot \mathbf{F}(\mathbf{Q}) = \nabla \cdot \mathbf{F}_v(\mathbf{Q}, \nabla \mathbf{Q}),$$

$$\mathbf{Q} = \begin{pmatrix} \rho \\ \rho \mathbf{u} \\ E \end{pmatrix}, \quad \mathbf{F} = \begin{pmatrix} \rho \mathbf{u} \\ \rho \mathbf{u} \mathbf{u} + p \mathbf{I} \\ (E + p) \mathbf{u} \end{pmatrix}, \quad \mathbf{F}_v = \begin{pmatrix} 0 \\ \sigma \\ \sigma \cdot \mathbf{u} - \mathbf{q} \end{pmatrix}$$

Viscous stress tensor:

$$\sigma = \mu(\nabla \mathbf{u} + (\nabla \mathbf{u})^T) - (2/3)(\nabla \cdot \mathbf{u}) \mathbf{I}$$

Heat flux: $\mathbf{q} = -k \nabla T$

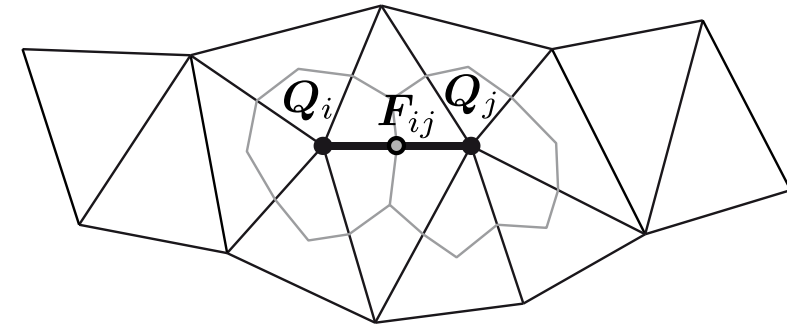
Ideal gas: $p = \rho R_{sp} T, \quad \varepsilon = R_{sp} T / (\gamma - 1)$

Viscous flux approximation:

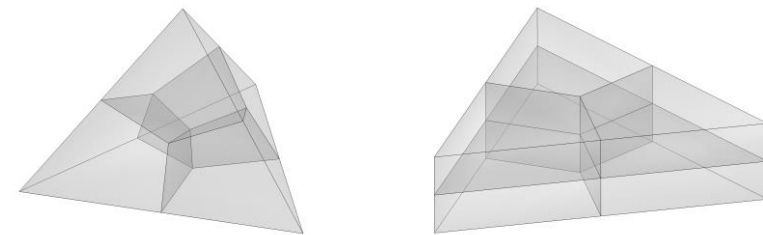
Bakhvalov P.A. Method of local element splittings for diffusion terms discretization in edge-bases schemes // Keldysh Institute Preprints. 2020. №79. 43p.

Node-centered barycentric cells:

2D)



3D)



Finite-volume method:

$$V_i \frac{d\mathbf{Q}_i}{dt} + \sum_{j \in N_1(i)} \mathbf{F}_{ij} \cdot \mathbf{s}_{ij} = F_{i,v}$$

Convective flux approximation by Roe method:

$$\mathbf{F}_{ij} = \frac{1}{2} (F(\mathbf{Q}_{ij}^R) + F(\mathbf{Q}_{ij}^L)) \cdot \mathbf{n}_{ij} - \frac{1}{2} |A_{ij}| (\mathbf{Q}_{ij}^R - \mathbf{Q}_{ij}^L)$$

To obtain Q_{ij}^L, Q_{ij}^R EBR schemes employ straight-line edge-based reconstruction: $Q_{ij}^L = R_{ij}^L\{Q\}, Q_{ij}^R = R_{ij}^R\{Q\}$.

In terms of divided differences

$$\Delta_m^L\{Q\} = \frac{Q_{m+1} - Q_m}{|\mathbf{r}_{m+1} - \mathbf{r}_m|}, \Delta_m^R\{Q\} = \Delta_{-m}^L\{Q\},$$

the corresponding reconstruction operators take the form:

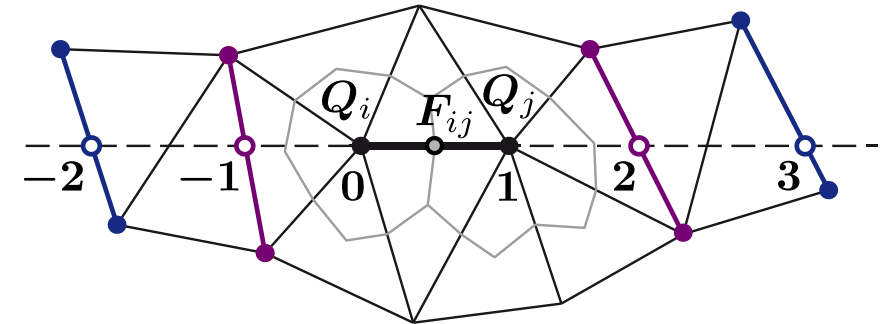
$$R_{ij}^L\{Q\} = Q_i + \frac{|\mathbf{r}_i - \mathbf{r}_j|}{2} \sum_m \beta_m \Delta_m^L\{Q\},$$

$$R_{ij}^R\{Q\} = Q_j - \frac{|\mathbf{r}_i - \mathbf{r}_j|}{2} \sum_m \beta_m \Delta_m^R\{Q\},$$

where values of β_i coefficients define concrete scheme from EBR family. Input values for the reconstruction are provided by linear interpolation

Abalakin I.V., Bakhvalov P.A., Kozubskaya T.K. Edge-based reconstruction schemes for unstructured tetrahedral meshes // Int. J. Numer. Methods Fluids. 2016. V. 81. № 6. P. 331–356.

EBR5 reconstruction stencil:



EBR5 (5-th order accuracy on translation-invariant meshes):

$$\beta_{-2} = -1/15, \beta_{-1} = 11/30, \\ \beta_0 = 4/5, \beta_1 = -1/10$$

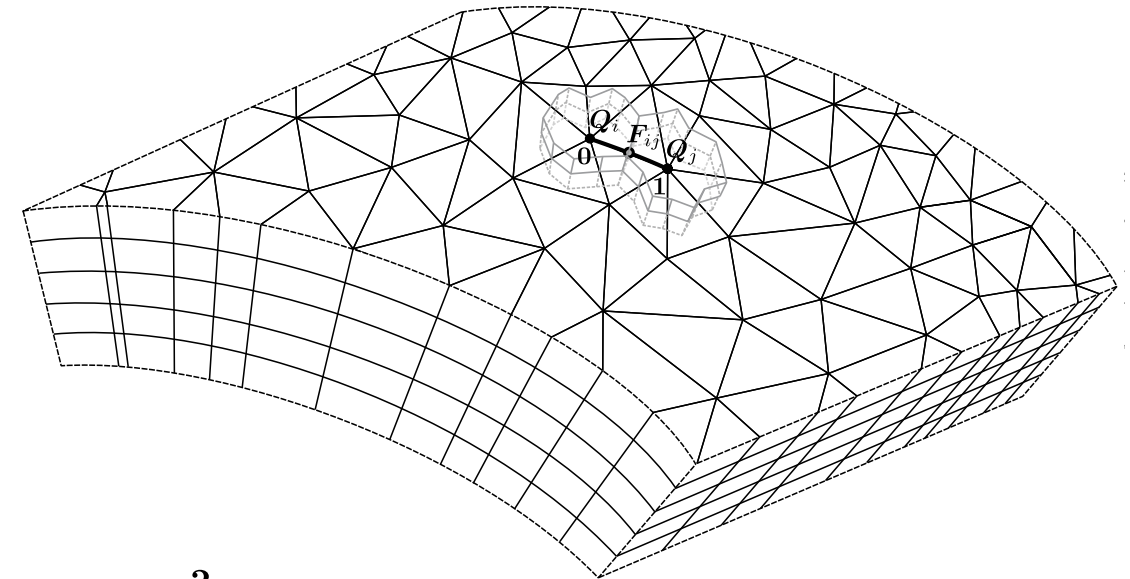
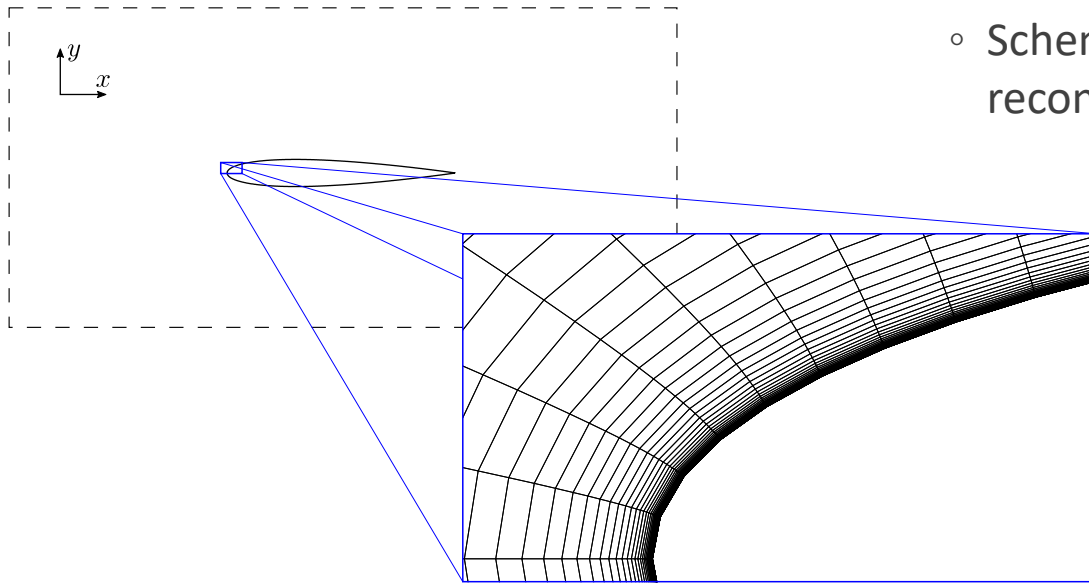
EBR3 (3-rd order accuracy on translation-invariant meshes):

$$\beta_{-1} = 1/3, \beta_0 = 2/3, \\ \beta_{-2} = 0, \beta_1 = 0$$

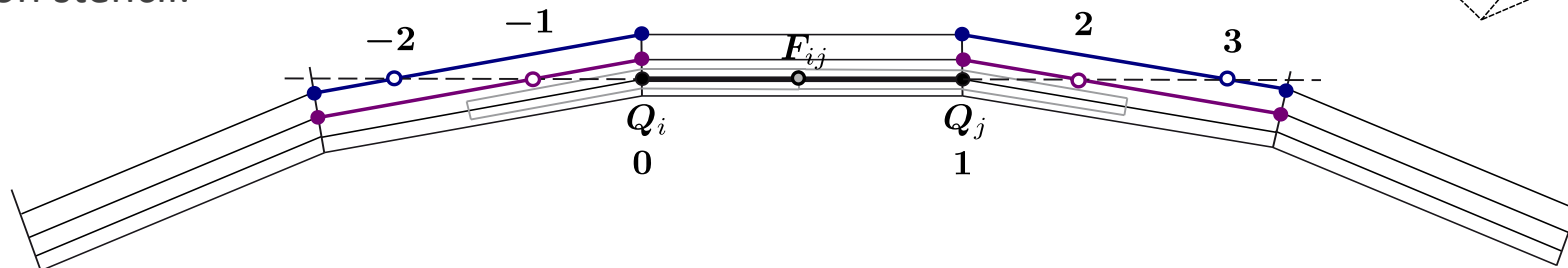
- Highly anisotropic
- Structured or prismatic

EBR straight-line reconstructions on such meshes may lead to

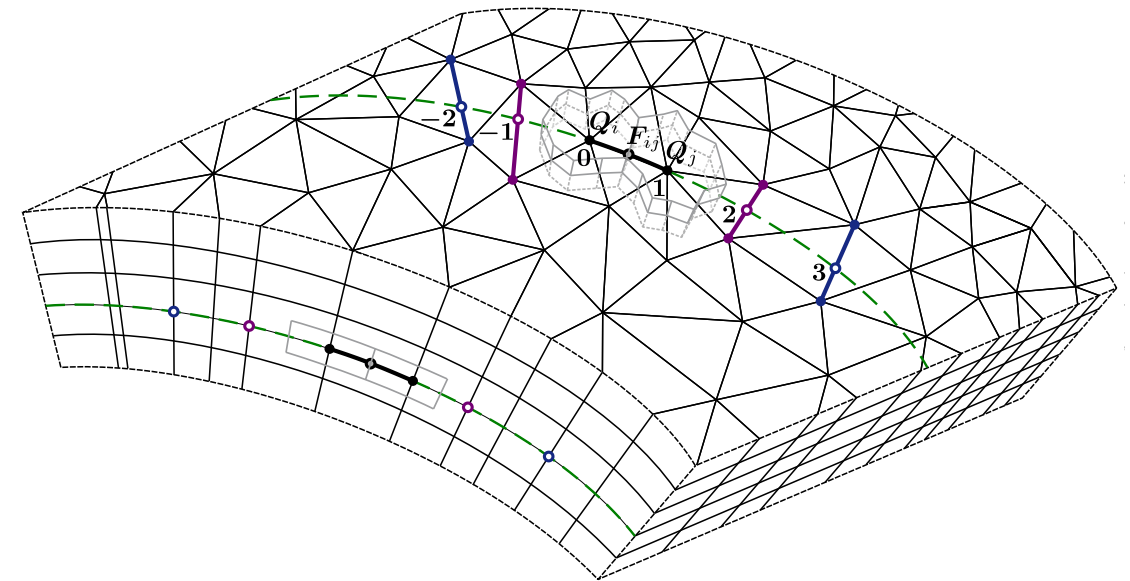
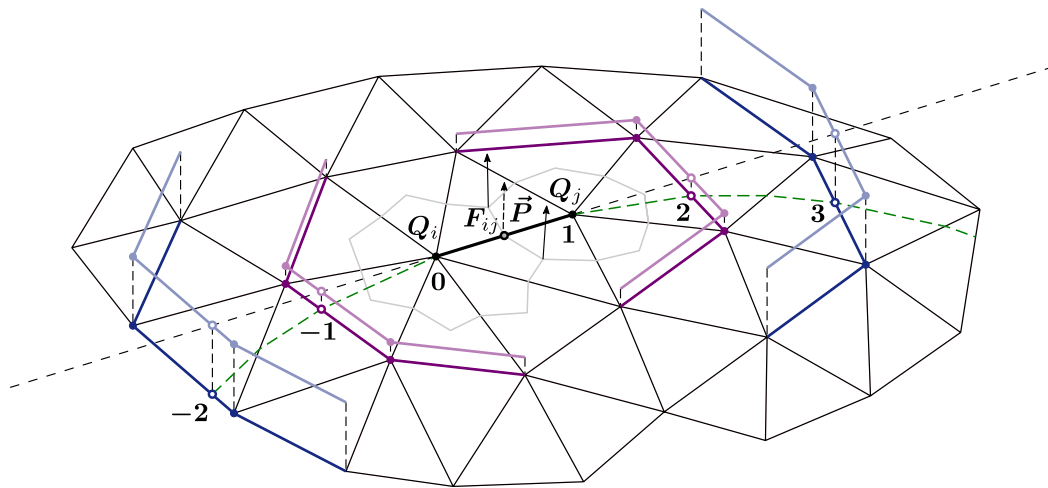
- Accuracy loss because nodes of reconstruction stencil are located in different boundary layer zones
- Scheme instability issues due to the distance imbalance between reconstruction nodes



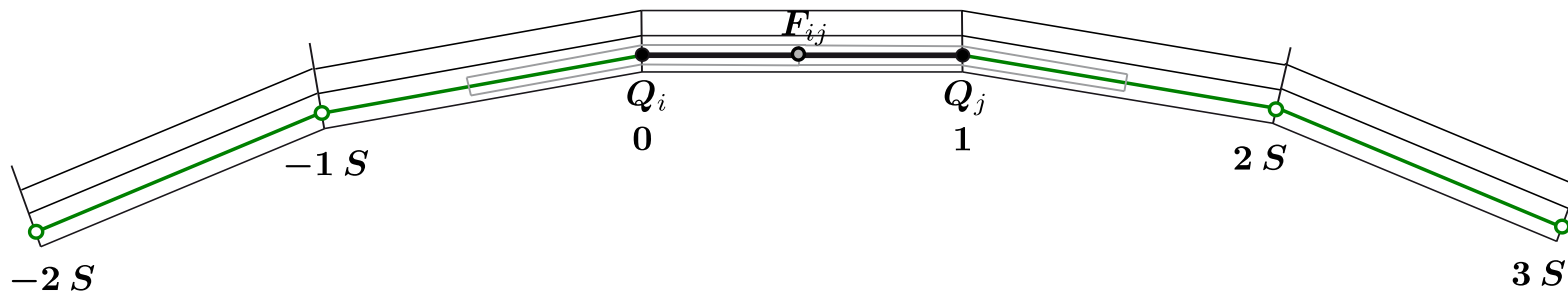
EBR5 reconstruction stencil:



- EBR IJK – if mesh is structured, use structural neighboring nodes for reconstructions
- EBR PL – if mesh is prismatic, define the projection plane that is orthogonal to prismatic layer and contain considering edge, project all neighboring nodes and edges of needed order to this plane, find nodes of standard EBR reconstruction on the plane, project these nodes back to prismatic layer and calculate all required reconstructions

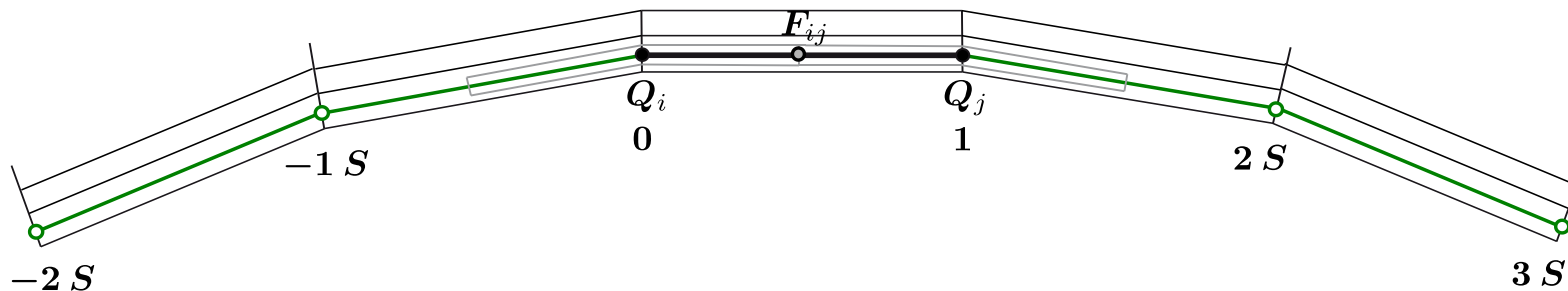


EBR5 IJK / PL reconstruction stencil:



1. Not all areas of structured or prismatic mesh provide advantages in accuracy and stability when using EBR IJK or EBR PL. Switching to the standard EBR scheme on sharp corners should be implemented.
2. If there are no enough nodes to build EBR5 IJK / PL reconstruction for the considering edge, it is reasonable to make an attempt to build EBR3 IJK / PL reconstruction. This practice may increase scheme accuracy and stability near sharp corners and interfaces between prismatic and unstructured mesh regions.
3. To make creation process of EBR PL reconstructions fast and straightforward, it is useful to preliminary mark up all layers of prismatic mesh.

EBR5 IJK / PL reconstruction stencil:



Linearized Navier–Stokes equations for background field with parameters $\bar{\rho} = 1$, $\bar{\mathbf{u}} = 0$, $\bar{p} = 1 / \gamma$:

$$\frac{\partial \rho'}{\partial t} + \nabla \cdot \mathbf{u}' = 0,$$

$$\frac{\partial \mathbf{u}'}{\partial t} + \nabla p' = \frac{1}{\text{Re}} \left(\Delta \mathbf{u}' + \frac{1}{3} \nabla (\nabla \cdot \mathbf{u}') \right),$$

$$\frac{\partial (p' - \rho')}{\partial t} = \frac{1}{\text{Re Pr}} \Delta (\gamma p' - \rho').$$

For an infinite cylindrical domain $r < R$, $0 < \varphi < 2\pi$, $z \in \mathbb{R}$ and boundary conditions

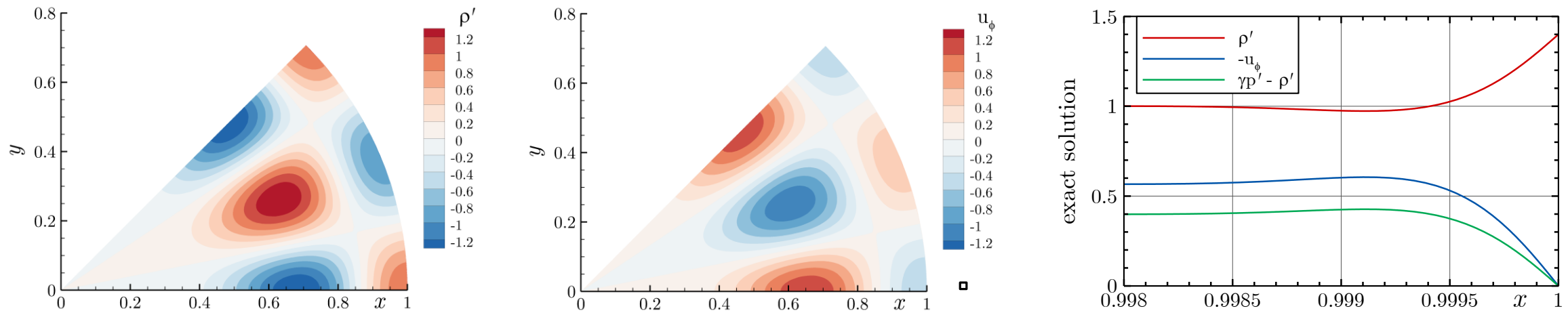
$$\mathbf{u}' \Big|_{r=R} = 0, \quad (\gamma p' - \rho') \Big|_{r=R} = 0,$$

it is possible to obtain exact solutions of a form

$$\mathbf{Q}'(r, \varphi, z, t) = \tilde{\mathbf{Q}}_m(r) e^{i\omega t + ikz + i\nu\varphi},$$

where $\mathbf{Q}' = (\rho', u'_r, u'_\varphi, u'_z, p')^T$, m – number of radial wave mode

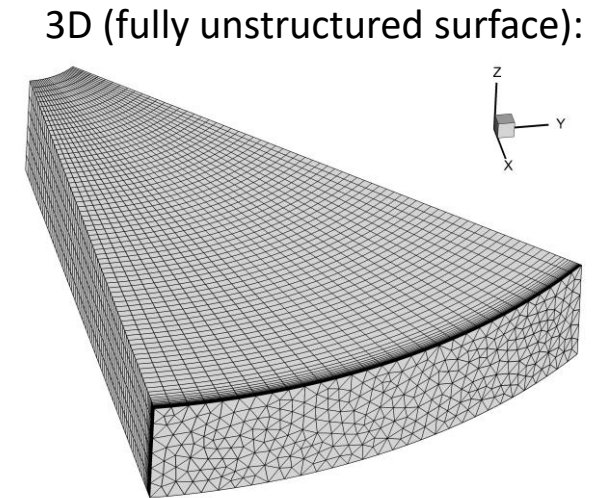
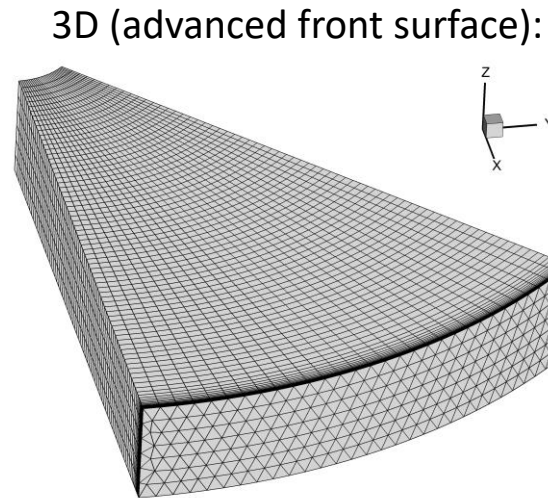
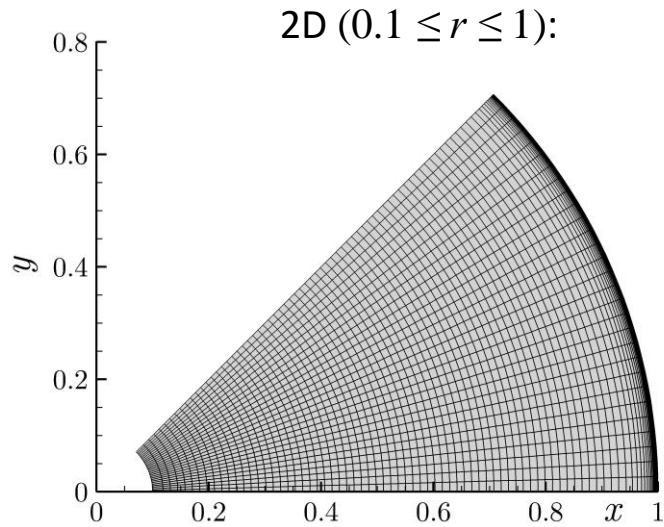
An example of the exact solution ($\text{Re} = 10^6$, $\text{Pr} = 1$, $\gamma = 1.4$, $R = 1$, $k = 0$, $\nu = 8$, $m = 1$):



Bakhvalov P.A. Sound wave in an infinite circular cylinder in the presence of viscosity and heat conductivity // Keldysh Institute Preprints. 2017. №135. 32 p.

CoESo (Collection of Exact Solutions, <http://caa.imamod.ru/index.php/research/CoESo>, <https://github.com/bahvalo/CoESo>)

- Mesh sequences are constructed for both two-dimensional and three-dimensional computations
- Computations are carried out by explicit EBR5 scheme and its curvilinear modifications with CFL = 1 until T = 20
- Curvilinear reconstructions increase accuracy of EBR5 scheme



Mesh type	N_φ	EBR5	Order	EBR5 IJK / PL	Order	Ratio
2D ($0.1 \leq r \leq 1$)	30	1.233×10^{-2}	—	1.552×10^{-3}	—	7.95
	60	2.742×10^{-3}	2.17	3.758×10^{-4}	2.05	7.30
	120	6.381×10^{-4}	2.10	9.352×10^{-5}	2.01	6.82
3D (advanced front surface)	30	1.040×10^{-2}	—	3.186×10^{-3}	—	3.26
	60	2.273×10^{-3}	2.19	6.178×10^{-4}	2.37	3.68
	120	5.159×10^{-4}	2.14	1.263×10^{-4}	2.29	4.09
3D (fully unstructured surface)	30	1.136×10^{-2}	—	5.589×10^{-3}	—	2.03
	60	2.823×10^{-3}	2.01	1.510×10^{-3}	1.89	1.87
	120	6.396×10^{-4}	2.14	2.784×10^{-4}	2.44	1.89

$$Re_c = 6 \cdot 10^6 \quad M_\infty = 0.15 \quad T_\infty = 300 \text{ K}$$

$$AOA = 0^\circ, 10^\circ, 15^\circ \quad \nu_t / \nu = 1$$

RANS with Spalart–Allmaras turbulence model

2D computational domain: $-500 \leq x/c, y/c \leq 500$

Airfoil leading edge at $(0, 0)$; c is chord length

3D computational domain: $-500 \leq x/c, y/c \leq 500$,

Airfoil leading edge at $(0, 0, z)$ $0 \leq z/c \leq 0.25$

2D meshes are structured quadrilateral near the airfoil and unstructured triangular in the rest domain, $y^+ < 1$

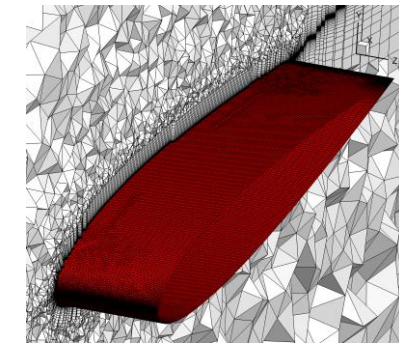
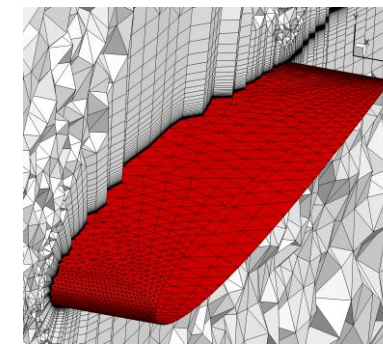
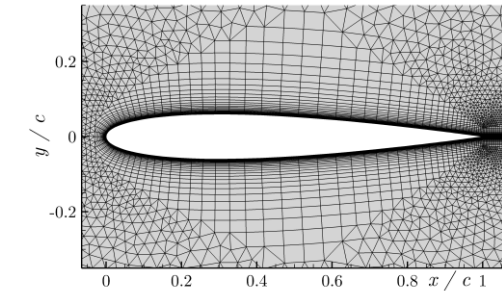
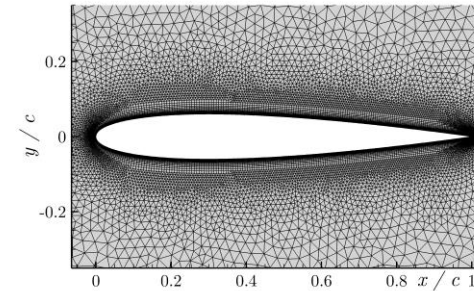
3D meshes are prismatic near the airfoil and unstructured tetrahedral in the rest domain, $y^+ < 1$

Boundary conditions on the airfoil:

$$\mathbf{u} = 0, \quad \partial T / \partial \mathbf{n} = 0, \quad \nu_t = 0$$

In-out conditions at $x/c = \pm 500$ and $y/c = \pm 500$

Periodic conditions in 3D at $z/c = 0$ and $z/c = 0.25$



x1

x4

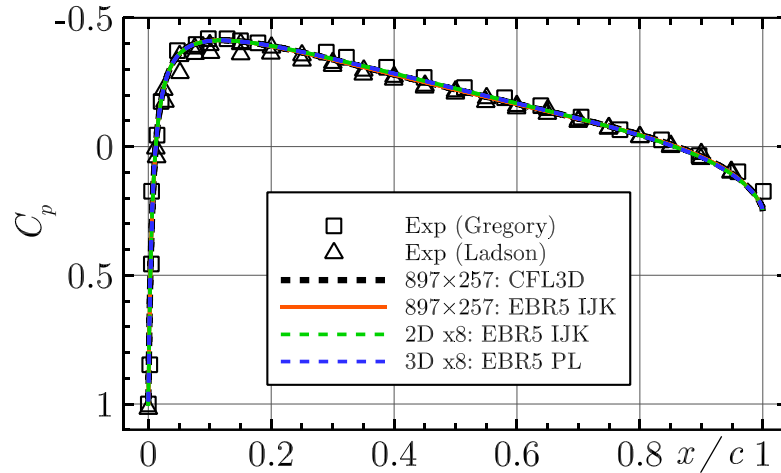
2D mesh	x1	x2	x3	x4	x8	897×257
N	5.5×10^4	5.1×10^4	6.9×10^4	8.3×10^4	8.4×10^4	2.3×10^5
N_{surf}	102	162	246	442	930	513

3D mesh	x1	x2	x3	x4	x8
N	5.2×10^5	8.0×10^5	1.4×10^6	2.9×10^6	9.7×10^6
N_{surf}	3.2×10^3	6.5×10^3	1.5×10^4	4.0×10^4	1.8×10^5
$N_{\text{surf}, z=0}$	102	162	246	442	930

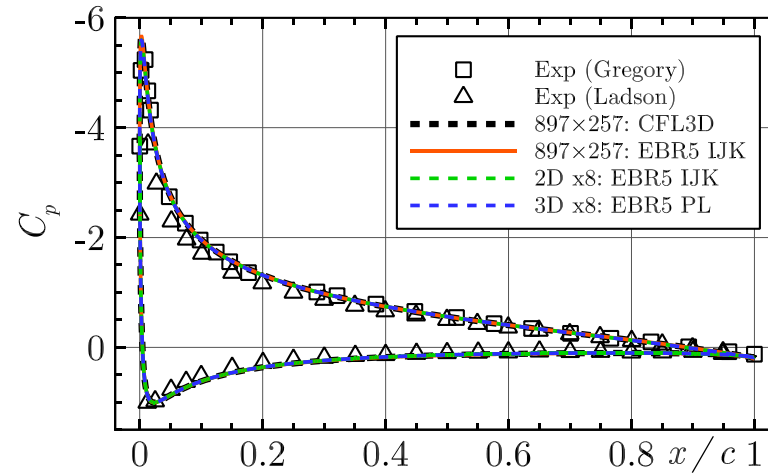
- Time integration (pseudotime): implicit first-order scheme resolved by Newton's method (1-2 iterations)
- Each Newton's iteration uses biconjugate gradient stabilized (BiCGSTAB) method with ILU0 preconditioner
- Computations are carried out until the convergence of
 - total energy (absolute residual)
 - turbulent viscosity (absolute residual)
 - drag coefficient
 - lift coefficient
- On coarse meshes standard EBR schemes required additional stabilization. For this purpose the limitation of allowable distances ratio inside reconstruction stencil was applied:
 - if maximum distances ratio in some EBR5 reconstruction stencil exceeds predefined limiting value EBR5 scheme switches locally to EBR3
 - if the maximum ratio still violates limitation the corresponding distances are set to the minimum values that satisfy the required condition

- Experimental data and reference CFL3D results are received from 2D NACA 0012 Airfoil Validation Case site (https://turbmodels.larc.nasa.gov/naca0012_val.html)

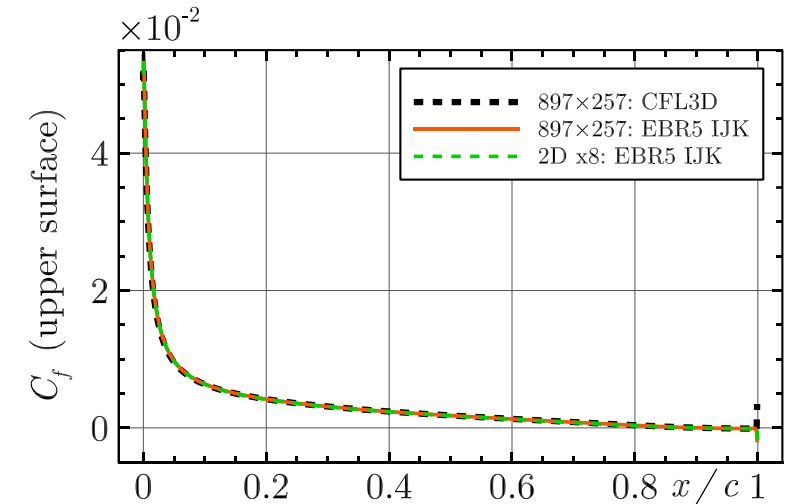
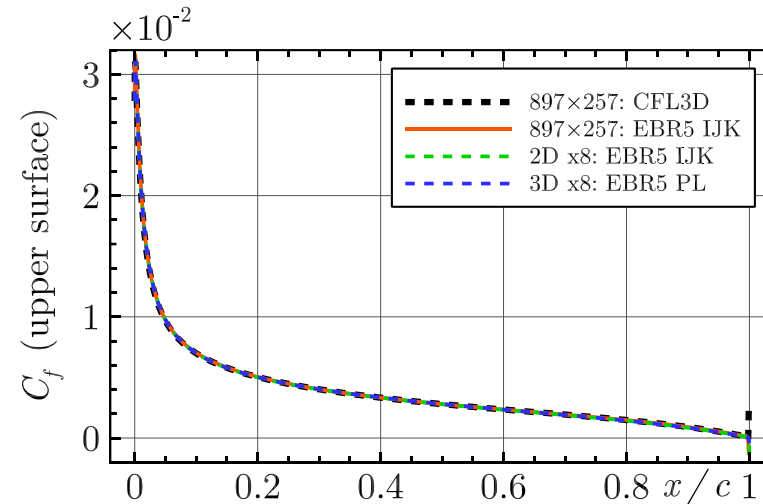
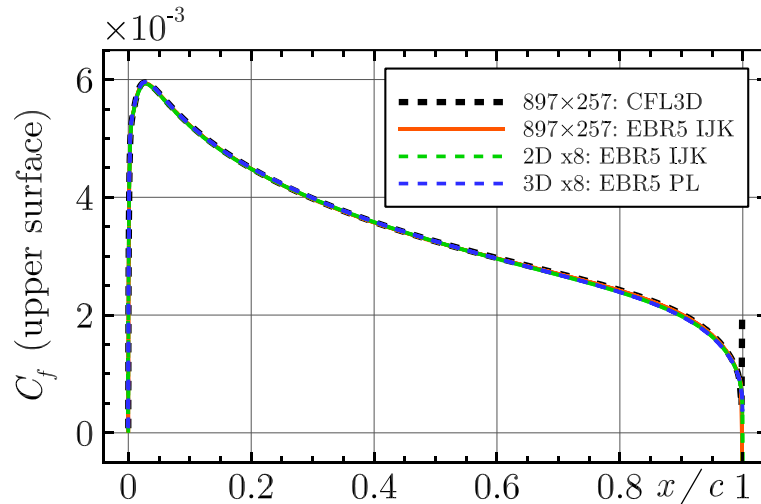
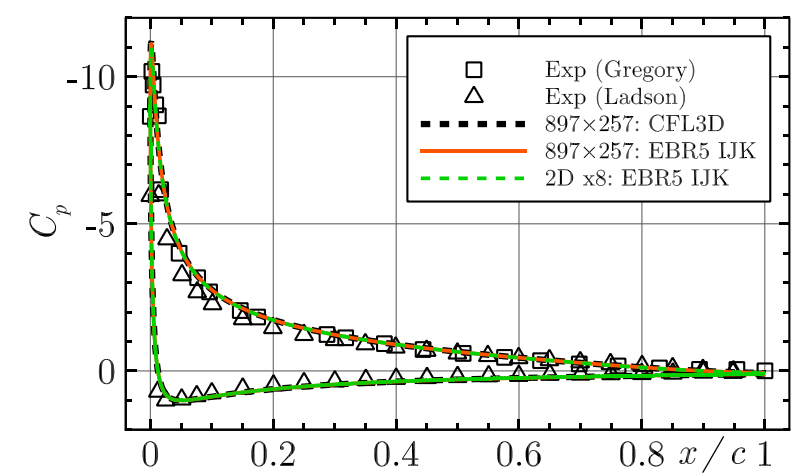
AOA = 0°



AOA = 10°



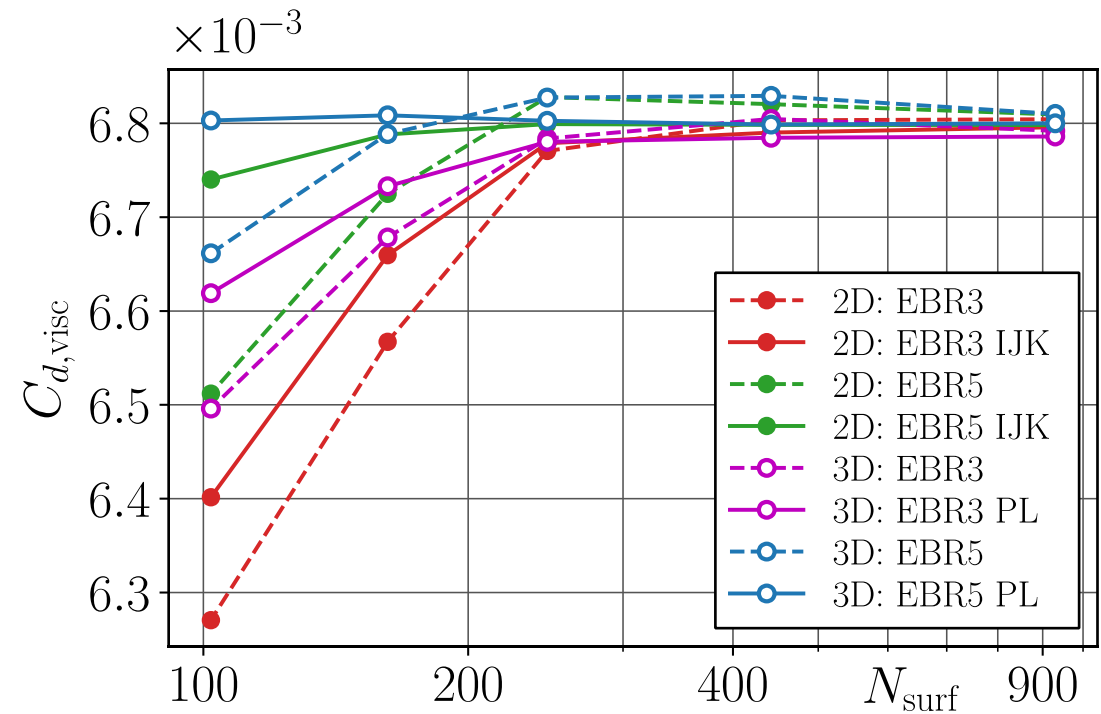
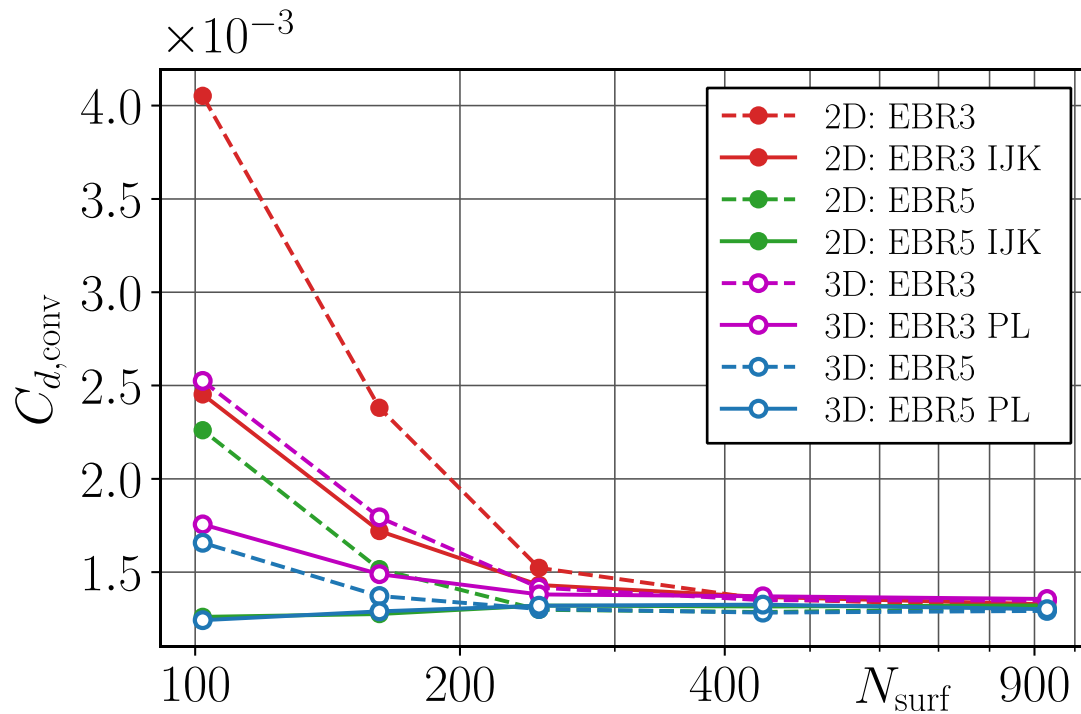
AOA = 15°



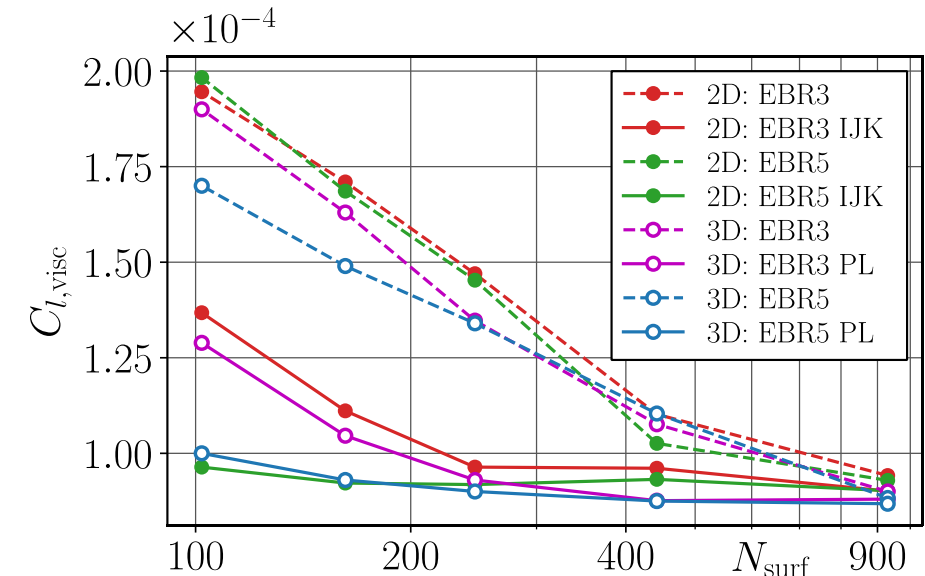
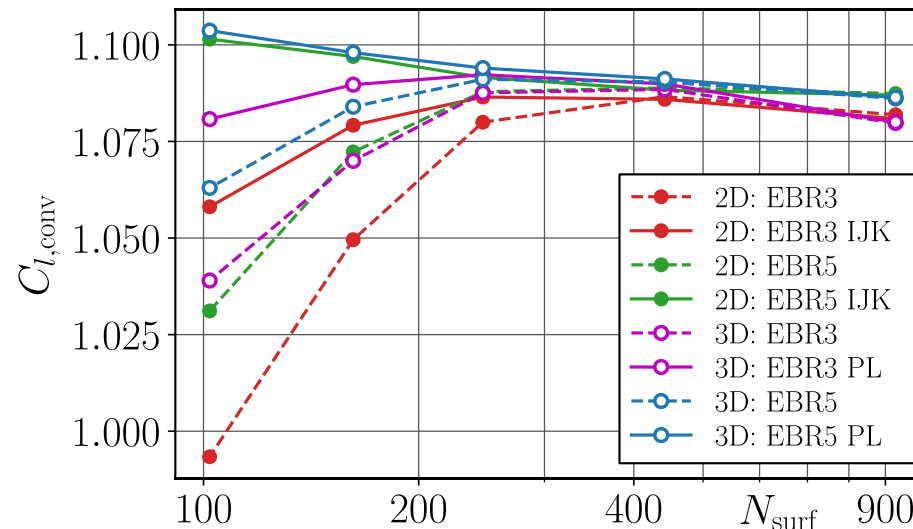
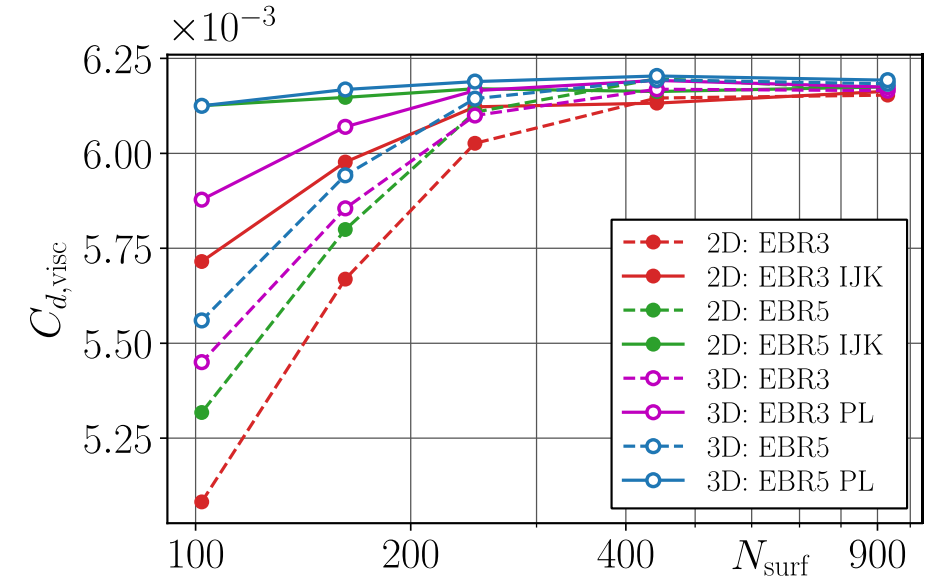
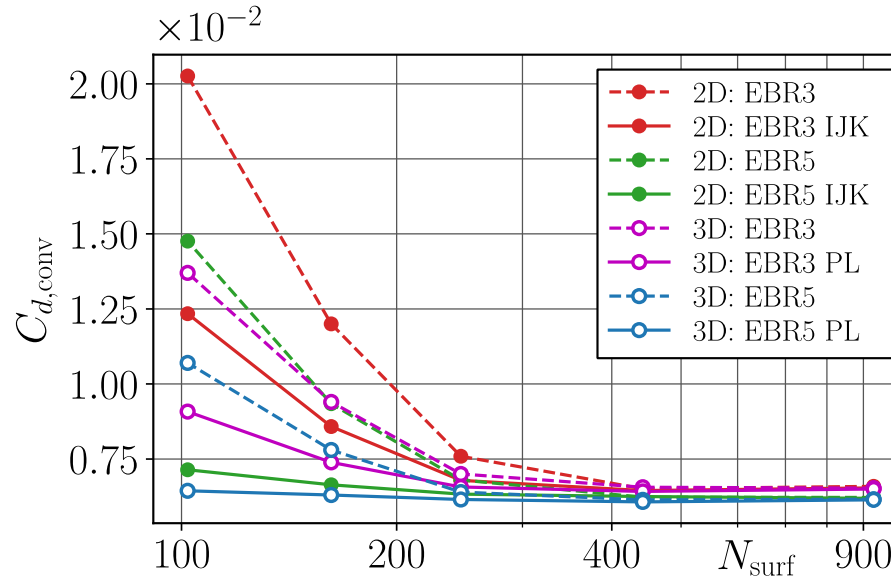
- Deviation of the obtained results from the mean reference values does not exceed
 - 1% for C_l at any AOA and for C_d at AOA 0° ,
 - 2% for C_d at AOA 10° ,
 - 4% for C_d at AOA 15°
- Difference between EBR5 schemes with straight-line and curvilinear reconstructions on 2D/3D x8 meshes does not exceed 0.1% for C_l and 1% for C_d

Mesh	Code / Scheme	$0^\circ: C_l$	$10^\circ: C_l$	$15^\circ: C_l$	$0^\circ: C_d$	$10^\circ: C_d$	$15^\circ: C_d$
897×257	CFL3D	~ 0	1.0909	1.5461	0.00819	0.01231	0.02124
897×257	FUN3D	~ 0	1.0983	1.5547	0.00812	0.01242	0.02159
897×257	NTS	~ 0	1.0891	1.5461	0.00813	0.01243	0.02105
897×257	EBR5	~ 0	1.0946	1.5437	0.00810	0.01264	0.02219
897×257	EBR5 IJK	~ 0	1.0940	1.5436	0.00810	0.01259	0.02203
2D x8	EBR5	~ 0	1.0875	1.5339	0.00811	0.01239	0.02179
2D x8	EBR5 IJK	~ 0	1.0871	1.5345	0.00812	0.01237	0.02166
3D x8	EBR5	~ 0	1.0862	–	0.00810	0.01234	–
3D x8	EBR5 PL	~ 0	1.0865	–	0.00810	0.01233	–

- EBR IJK and EBR PL provide more accurate results in comparison with straight-line EBR
- EBR5 IJK and EBR5 PL on the coarsest meshes give the integral values that are very close to the corresponding values on the fine meshes
- 3D case results are more accurate than the corresponding results in 2D

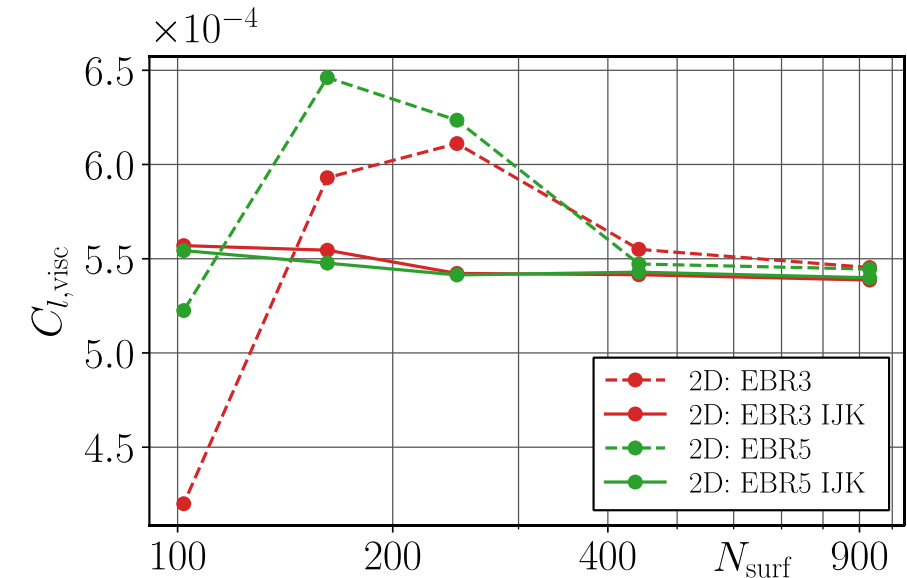
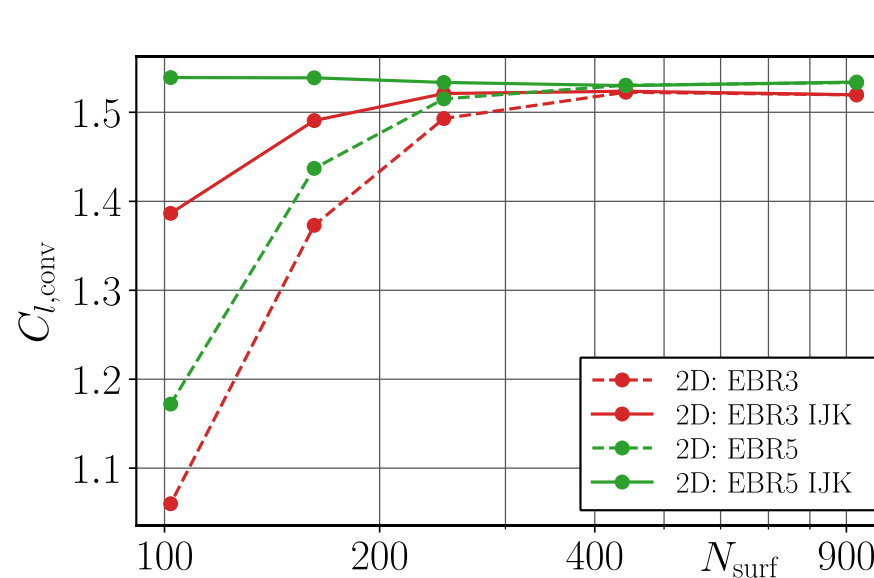
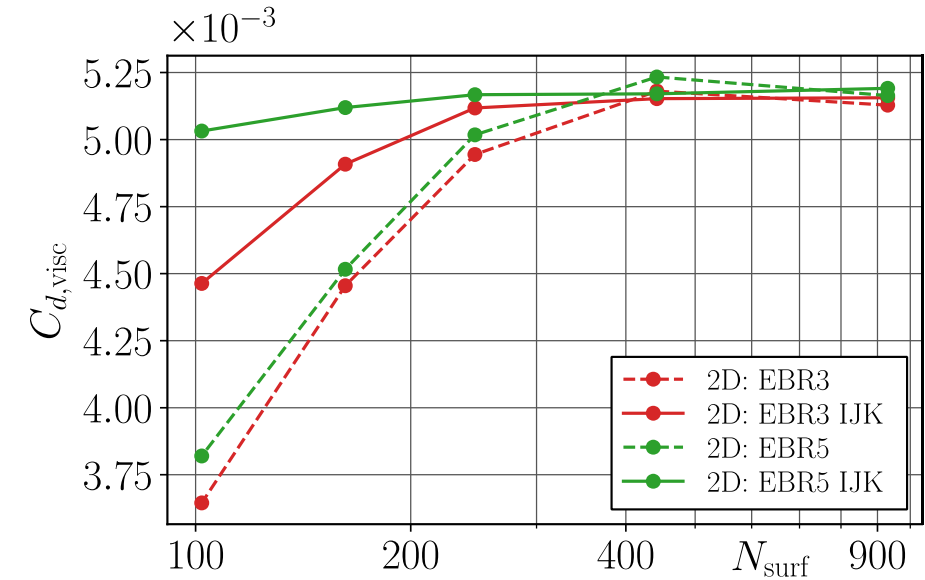
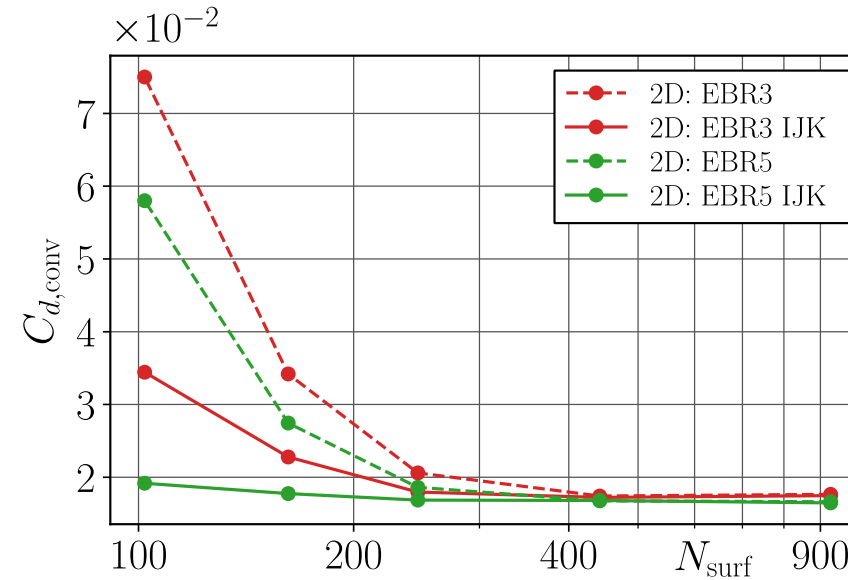


- EBR IJK and EBR PL provide more accurate results in comparison with straight-line EBR
- Even EBR3 IJK and EBR3 PL allow to obtain better results than straight-line EBR5
- EBR5 IJK and EBR5 PL on the coarsest meshes give the integral values that are very close to the corresponding values on the fine meshes
- 3D case results are more accurate than the corresponding results in 2D



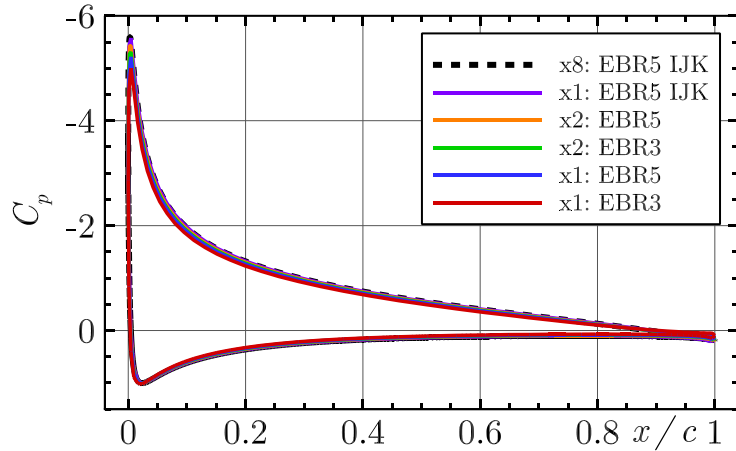
Advantages on coarse meshes: AOA = 15°

- EBR IJK provides more accurate results in comparison with straight-line EBR
- Even EBR3 IJK allows to obtain better results than straight-line EBR5
- EBR5 IJK on the coarsest meshes gives the integral values that are very close to the corresponding values on the finest mesh

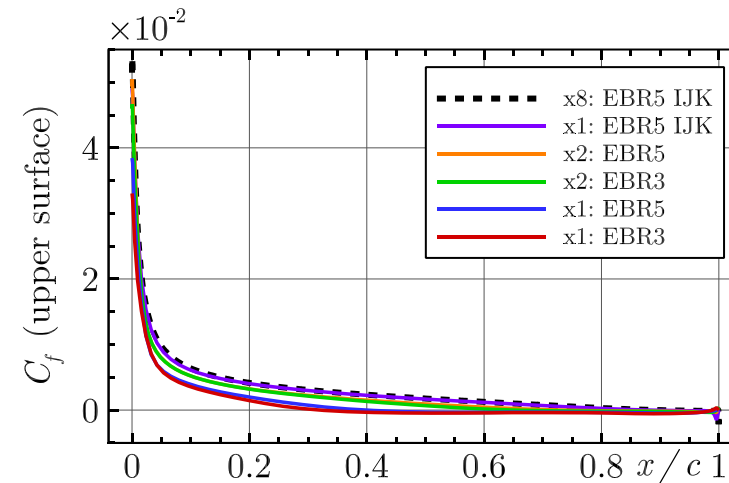
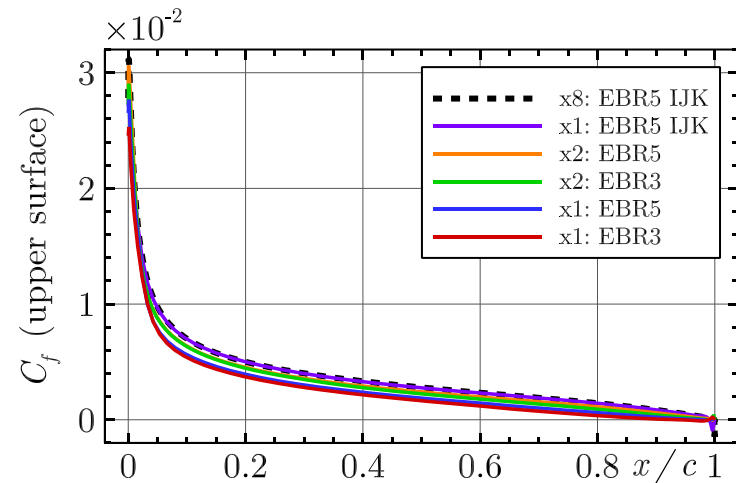
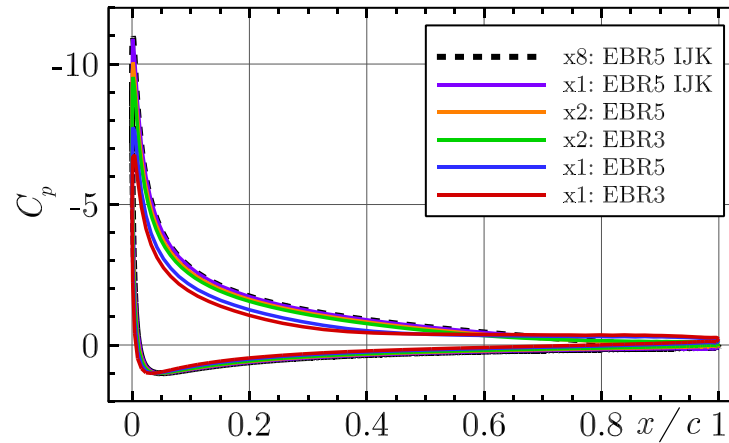


- Employing EBR5 IJK on the coarsest mesh is enough to obtain the good agreement with the results on the finest mesh
- Usage of straight-line reconstructions on coarse meshes may lead to valuable inaccuracies in flow separation region

AOA = 10°



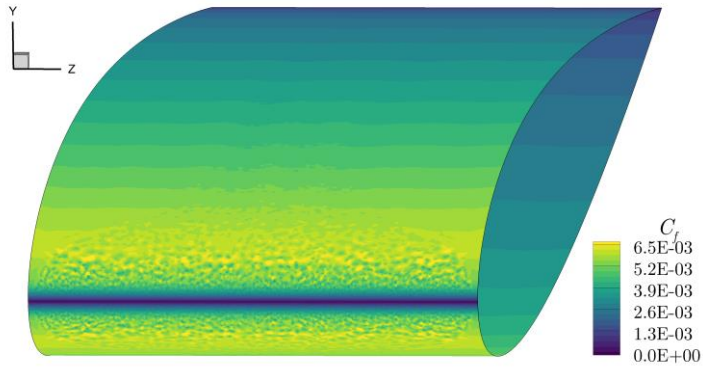
AOA = 15°



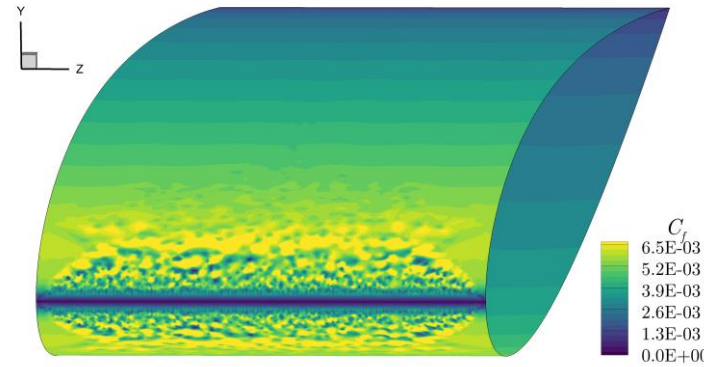
Mesh	Code / Scheme	10°	15°
897×257	CFL3D	no sep.	0.91
897×257	EBR5 IJK	no sep.	0.91
2D x8	EBR5 IJK	no sep.	0.90
3D x8	EBR5 PL	no sep.	–
2D x1	EBR5 IJK	no sep.	0.89
2D x2	EBR5	0.994	0.74
2D x2	EBR3	0.987	0.66
2D x1	EBR5	0.980	0.40
2D x1	EBR3	0.935	0.32
3D x1	EBR5	no sep.	–
3D x1	EBR3	0.973	–

- Usage of straight-line reconstructions may lead to valuable instabilities of friction coefficient
- AOA = 0° (the similar effects are observed for the EBR3 scheme and for others angles of attack)

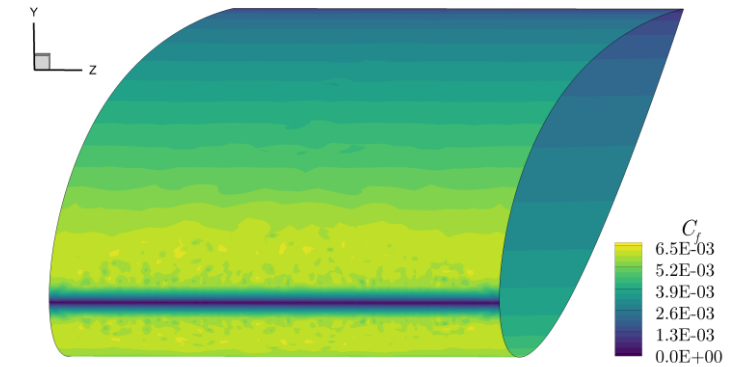
x8: EBR5



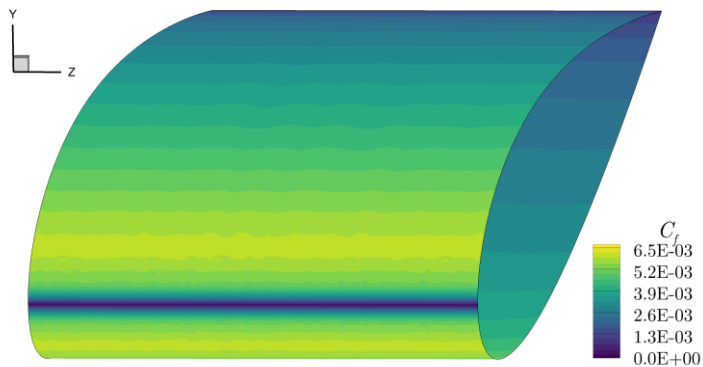
x4: EBR5



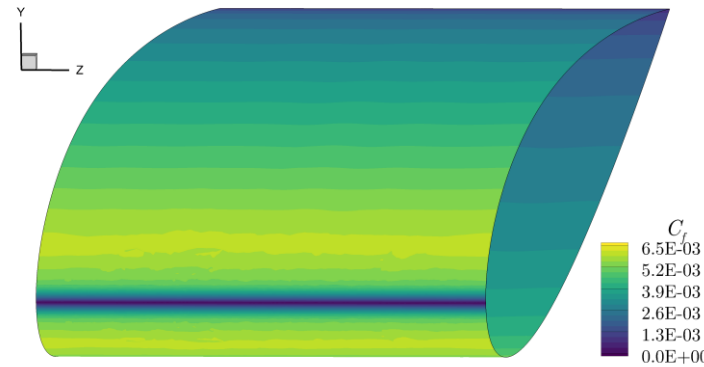
x3: EBR5



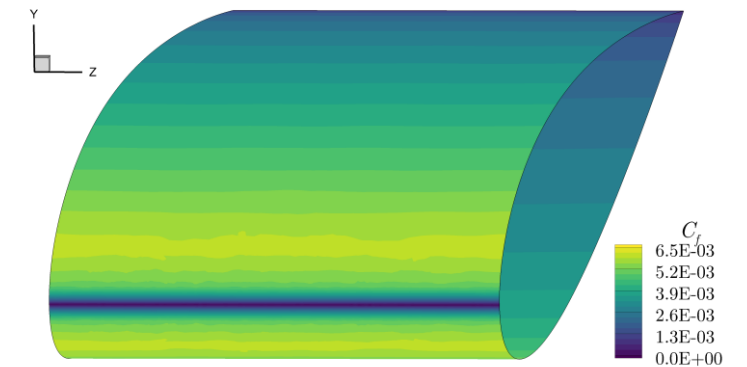
x8: EBR5 PL



x4: EBR5 PL



x3: EBR5 PL

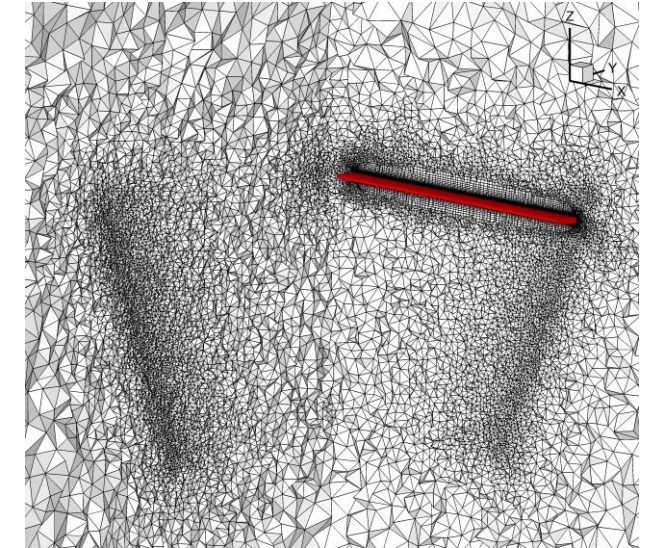
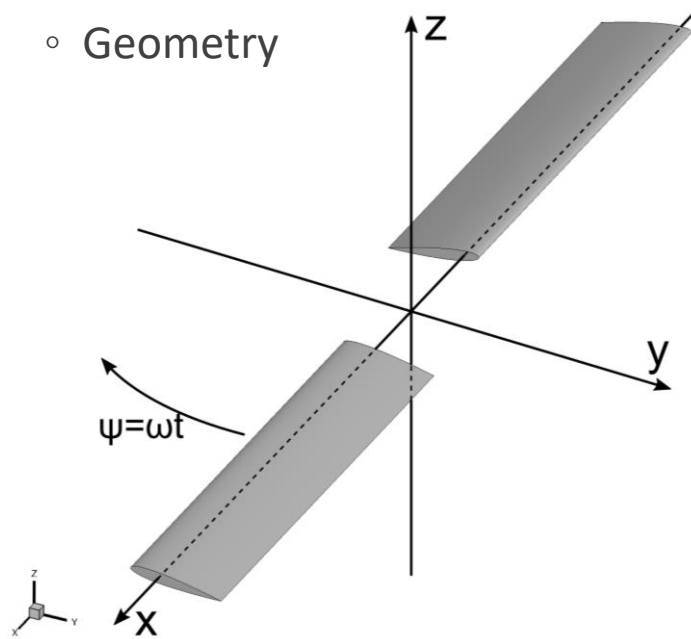


Caradonna–Tung problem

Case setup

Blades count	2
Rotor radius	1.143 m
Blade chord	0.1905 m
Blade base profile	NACA 0012
Pitch angle	8°
Flight regime	hover
Flight height	0 m

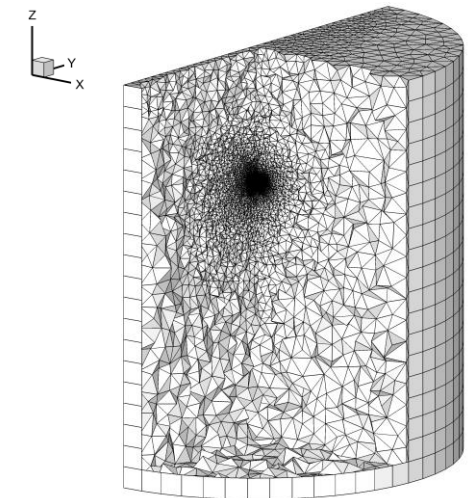
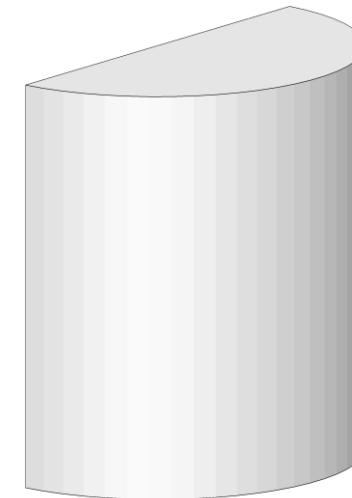
Geometry



Considered rotation speeds

RPM	M_{tip}	$Re_{c,tip}$	U_{tip}
650	0.23	9.8×10^5	78 m/s
1750	0.61	2.6×10^6	209 m/s
2300	0.80	3.4×10^6	275 m/s

- Computational domain with axial periodic
- domain radius: 30 m
- domain height: 60 m

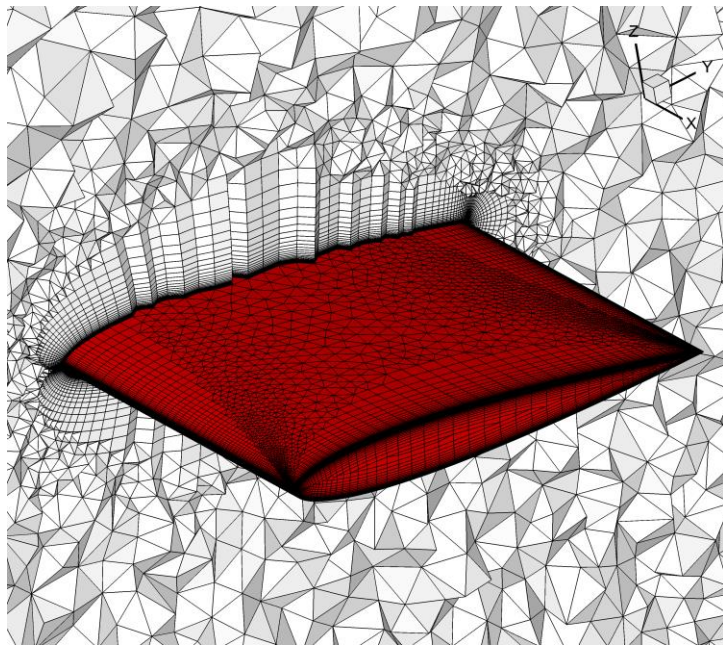


Caradonna F.X., Tung C. Experimental and Analytical Studies of a Model Helicopter Rotor in Hover. Technical report, NASA Technical Memorandum TM-81232, 1981

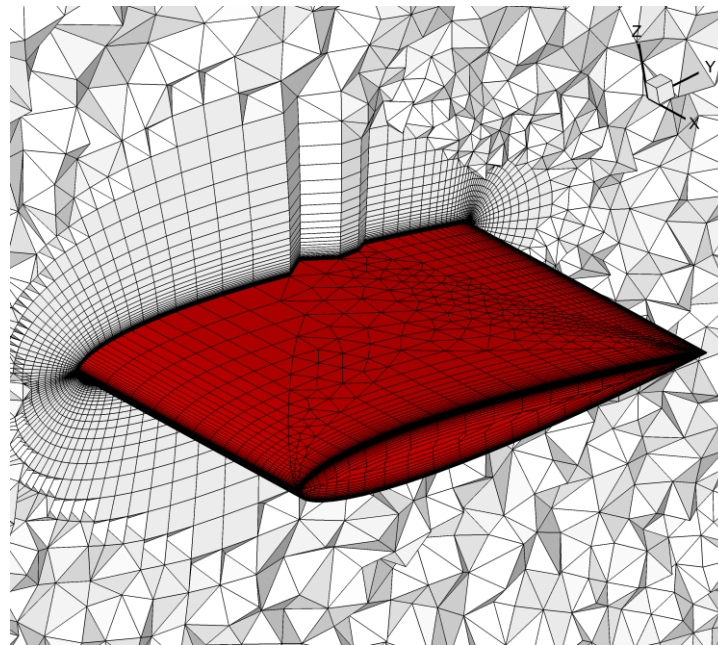
- RANS with Spalart–Allmaras turbulence model
- Fully turbulent flow
- $y^+ < 1$ in all cases
- Boundary conditions in analogy with NACA 0012 case
- Implicit EBR5 and EBR-WENO5 schemes with and without curvilinear reconstructions

Meshes	N	$N_{\text{leading edge}}$	$N_{\text{tip,upper}}$	$N_{\text{trailing edge}}$
x2	3.2M	300	80	300
x1	1.7M	90	50	150
x1c	1.3M	80	40	75

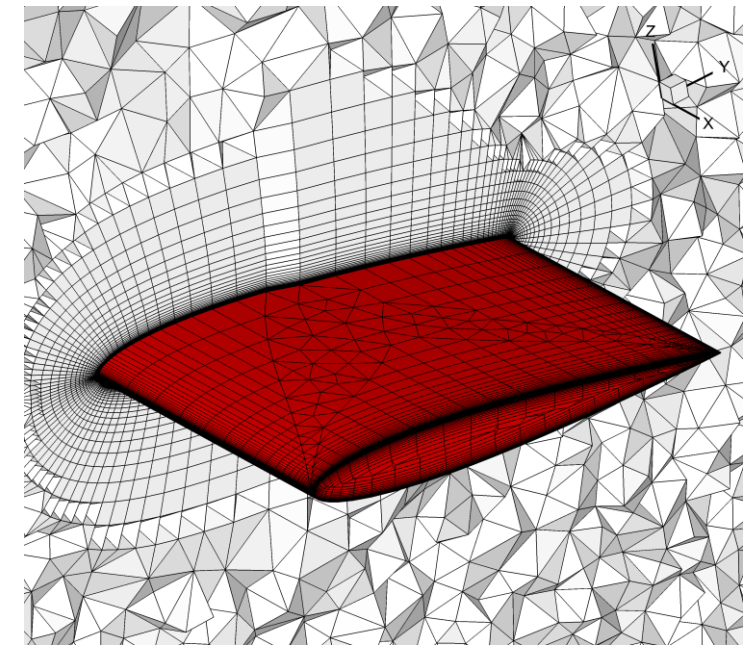
x2:



x1:



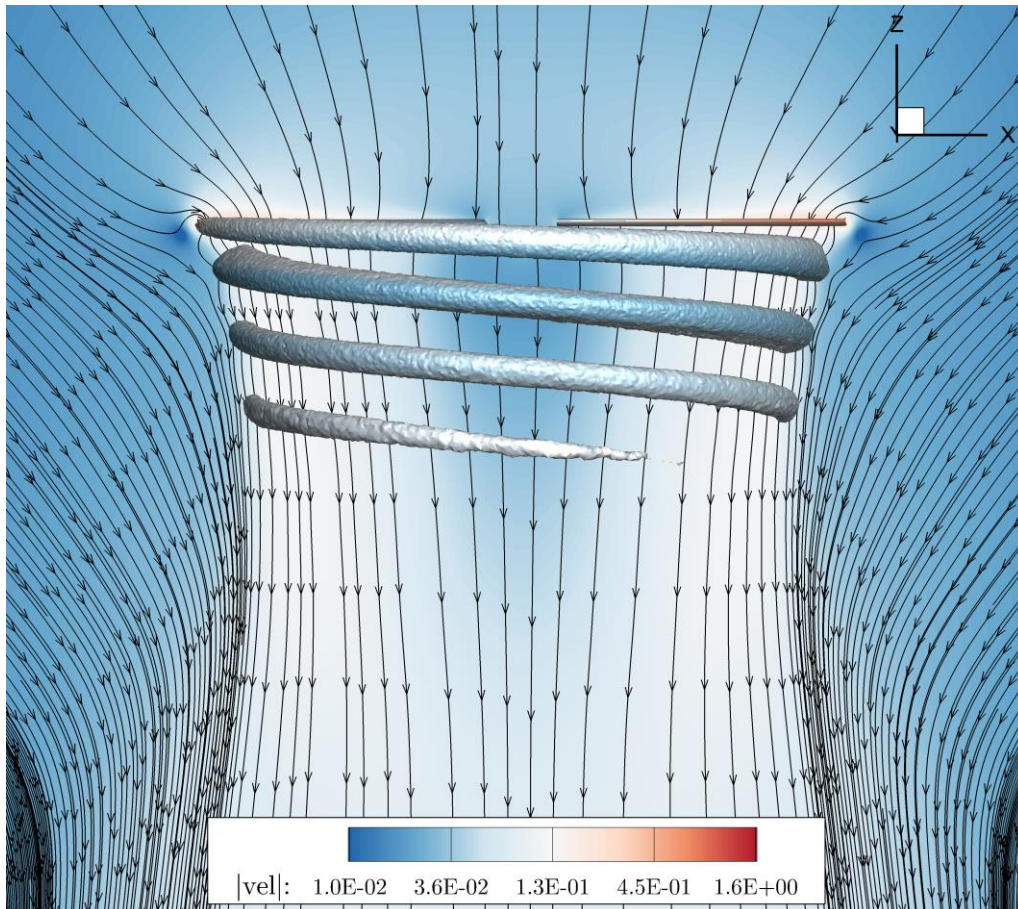
x1c:



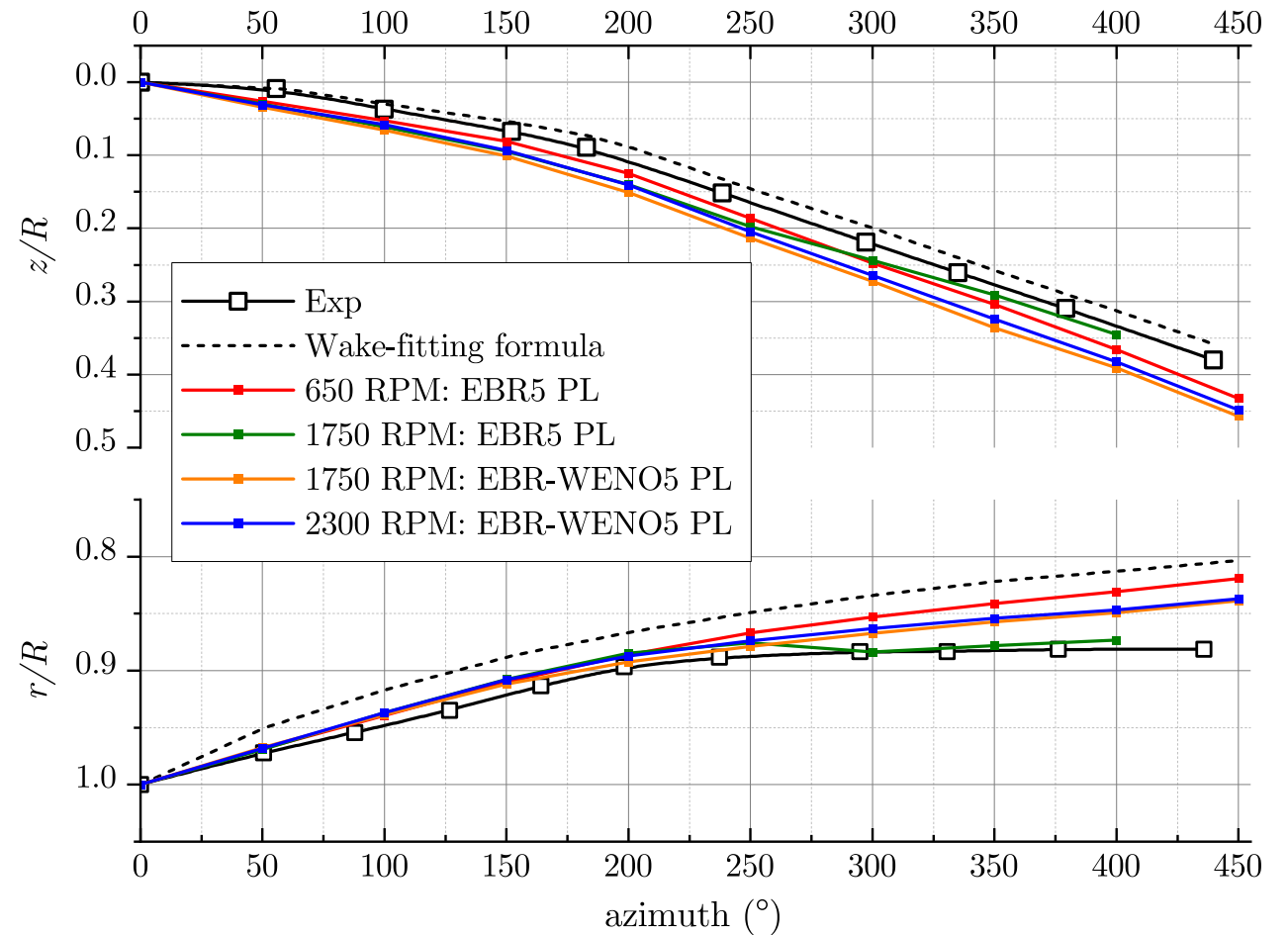
Bakhvalov P.A., Kozubskaya T.K. EBR-WENO scheme for solving gas dynamics problems with discontinuities on unstructured meshes // *Comput. Fluids*. 2017. V. 157. P. 312–324

Results obtained by EBR schemes with curvilinear reconstructions on mesh x2:

- 1750 RPM: EBR-WENO5 PL
- Streamlines within the plane $y = 0$
- Iso-surface corresponds to Q-criterion = 0.01

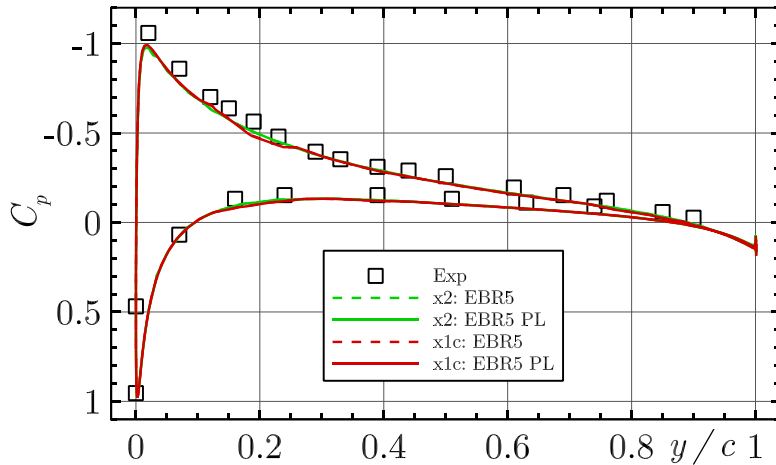


- Vortex position agree well with the experiment

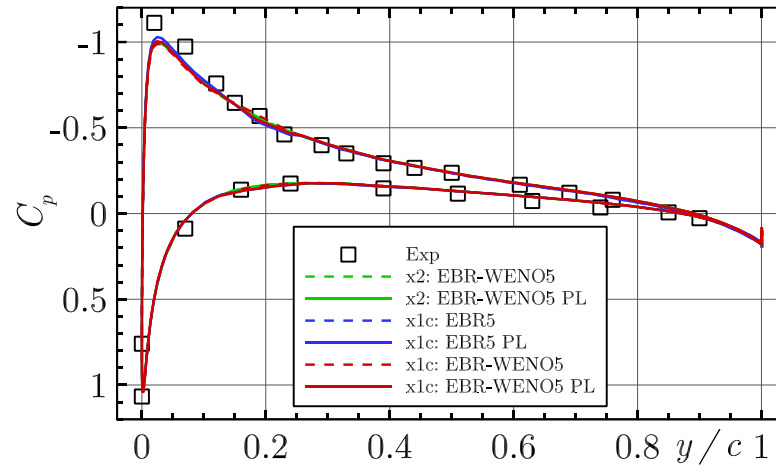


- Numerical results agree well with the experiment
- Curvilinear reconstructions have almost zero impact on pressure distribution

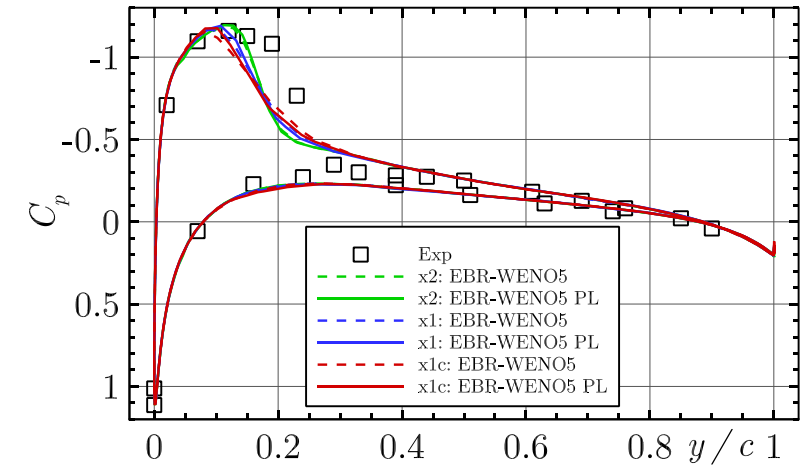
650 RPM (0.96L)



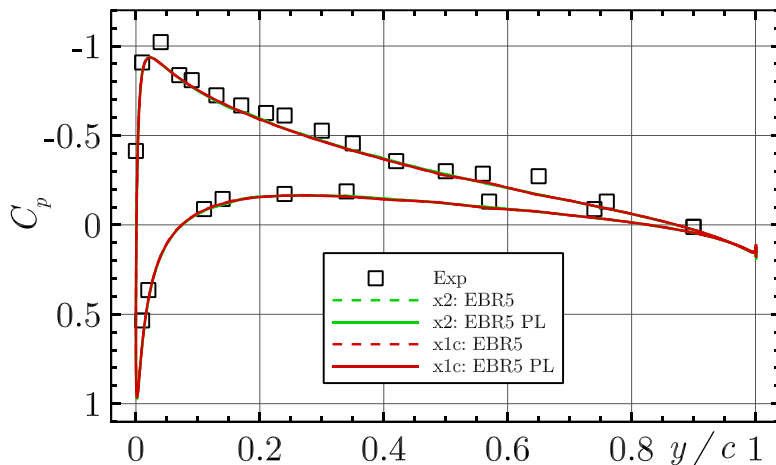
1750 RPM (0.96L)



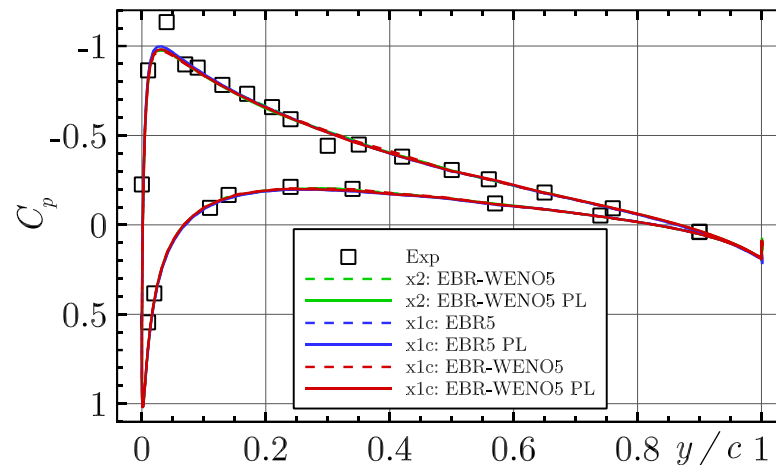
2300 RPM (0.96L)



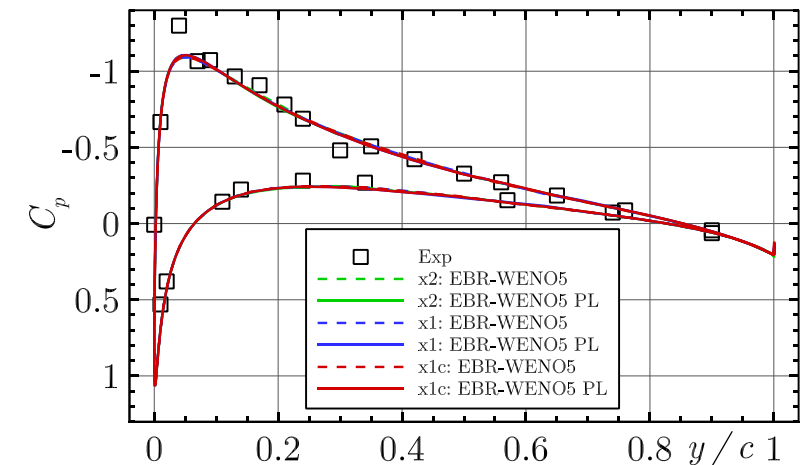
650 RPM (0.8L)



1750 RPM (0.8L)

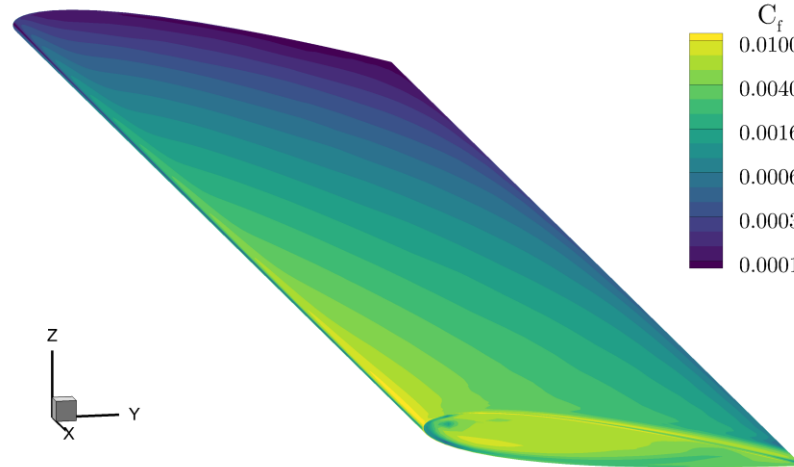


2300 RPM (0.8L)

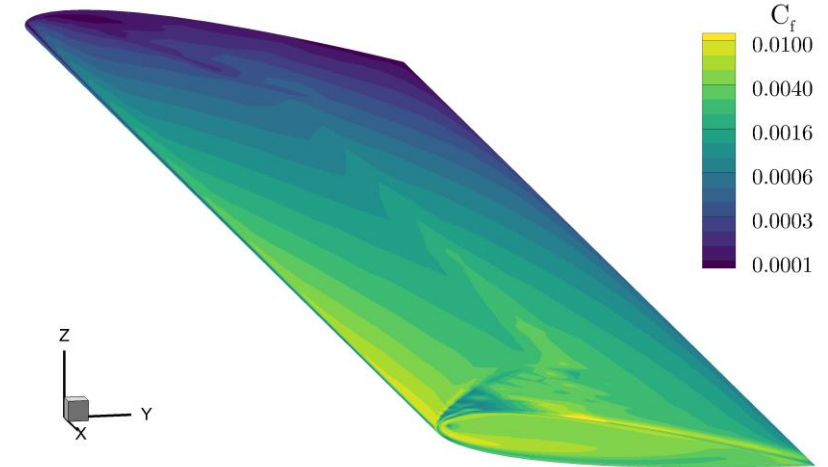


- EBR5 and EBR5 PL provide almost the same result but for stable computation process require approximately 10 times lower CFL than the CFL required by EBR-WENO5 or EBR-WENO5 PL

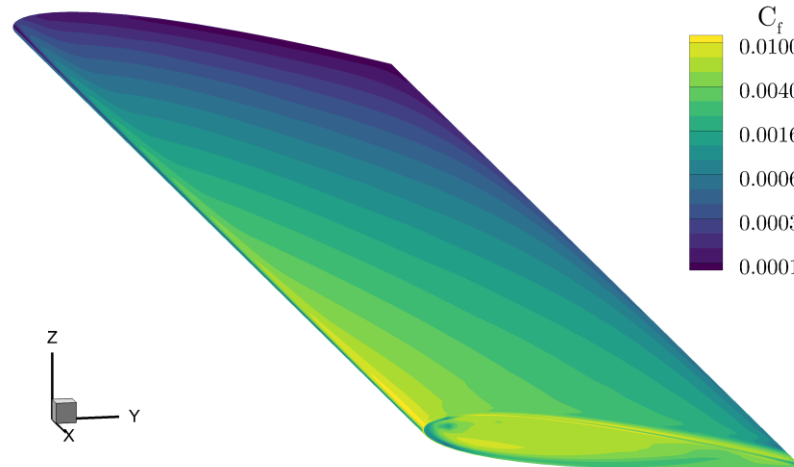
x1c EBR5



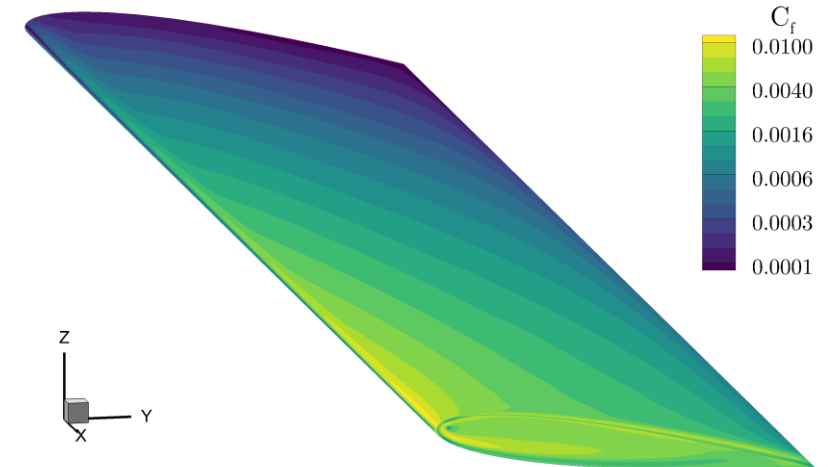
x1c EBR-WENO5



x1c EBR5 PL

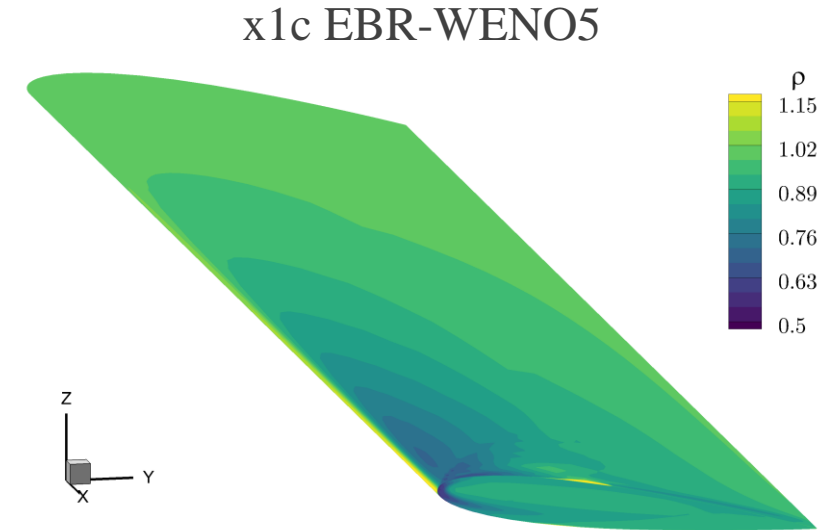
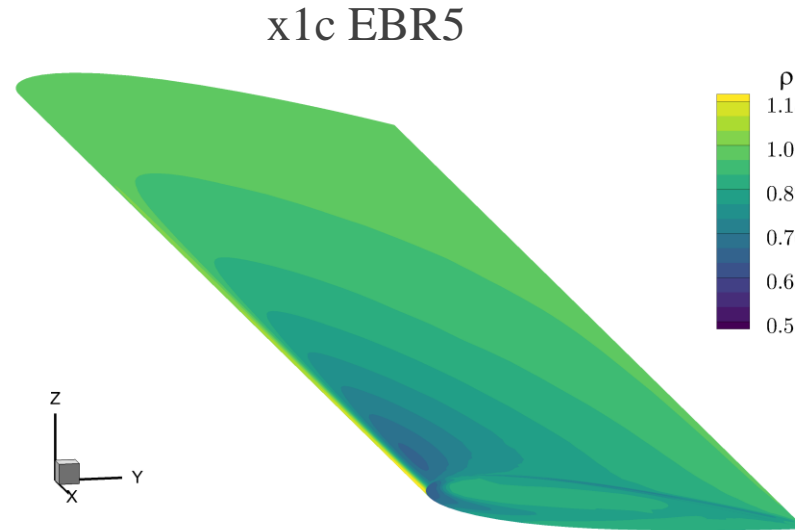


x1c EBR-WENO5 PL

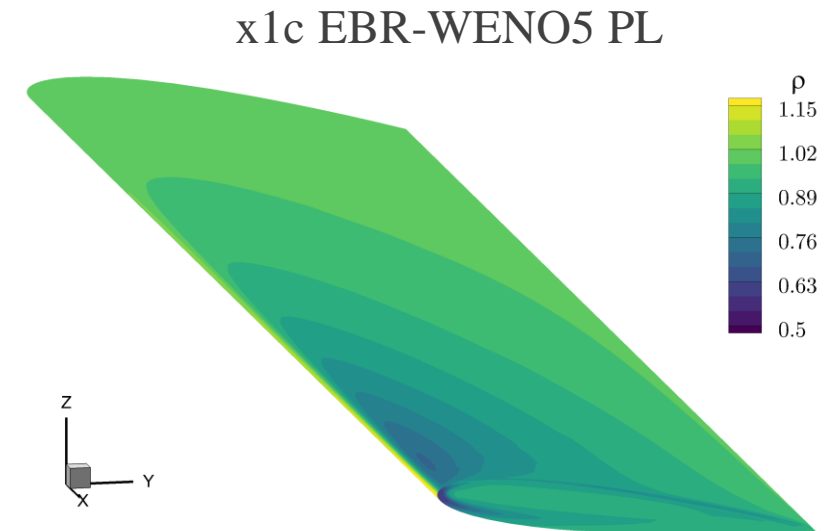
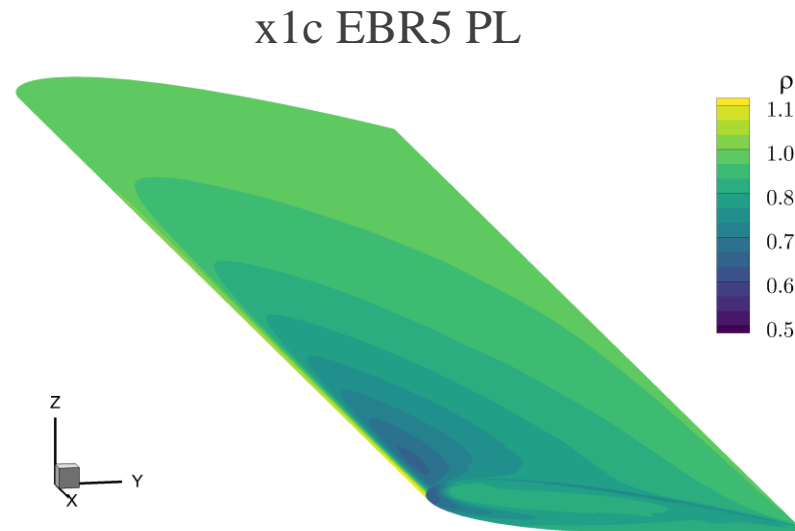


- EBR-WENO5 induces non-physical fluctuations that may be eliminated by using EBR-WENO5 PL

- EBR5 and EBR5 PL provide almost the same result but for stable computation process require approximately 40 times lower CFL than the CFL required by EBR-WENO5 or EBR-WENO5 PL

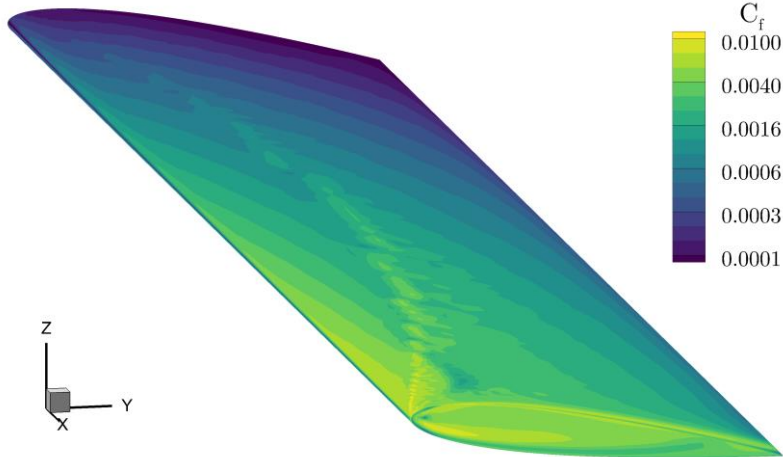


- EBR-WENO5 induces non-physical fluctuations that may be eliminated by using EBR-WENO5 PL

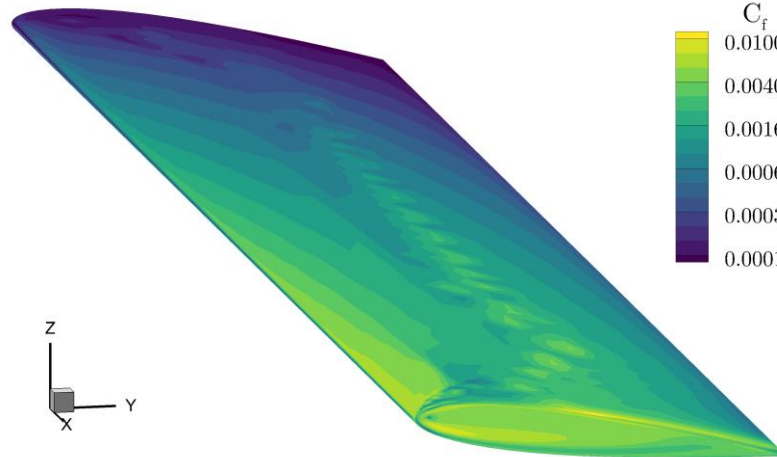


- EBR-WENO5 induces non-physical fluctuations that may be eliminated by using EBR-WENO5 PL

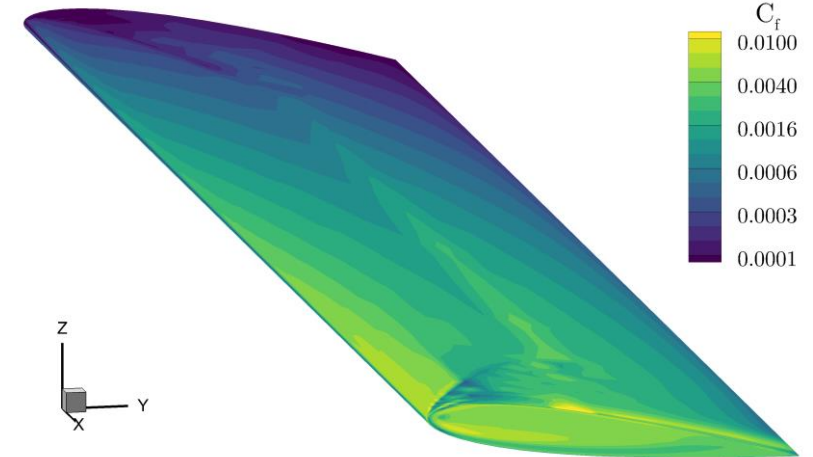
x2 EBR-WENO5



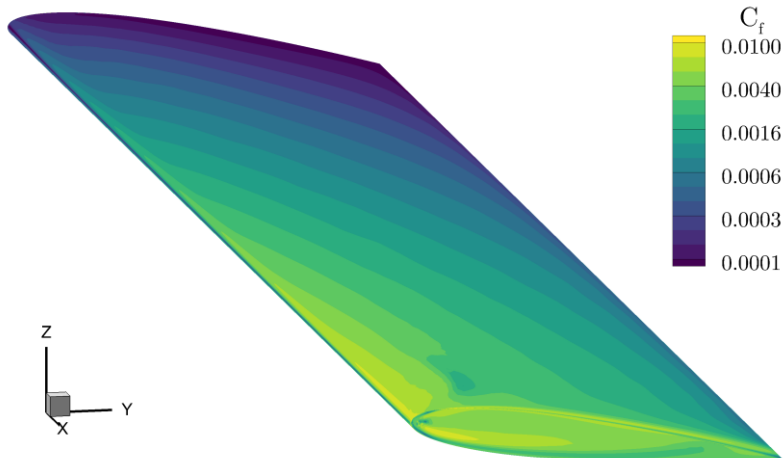
x1 EBR-WENO5



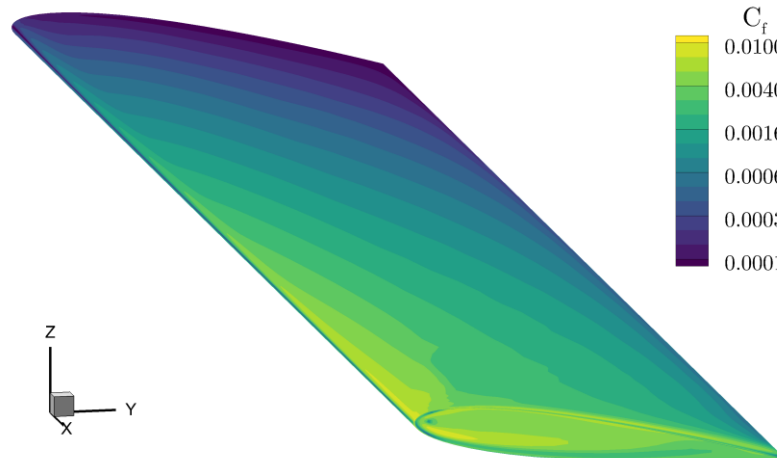
x1c EBR-WENO5



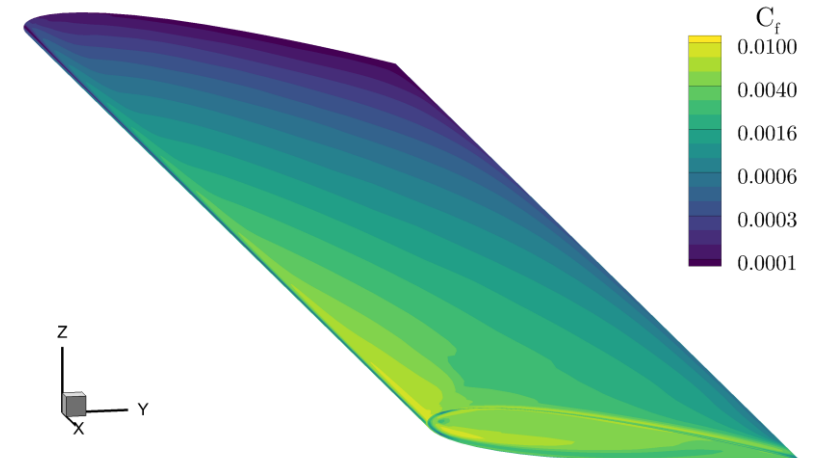
x2 EBR-WENO5 PL



x1 EBR-WENO5 PL

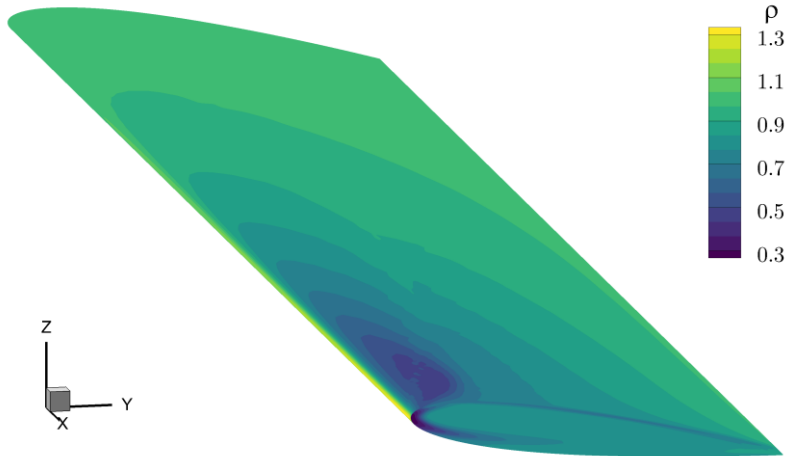


x1c EBR-WENO5 PL

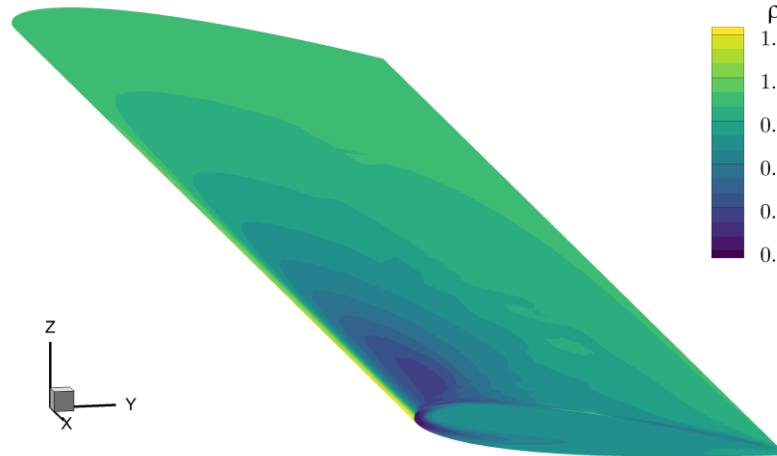


- EBR-WENO5 induces non-physical fluctuations that may be eliminated by using EBR-WENO5 PL

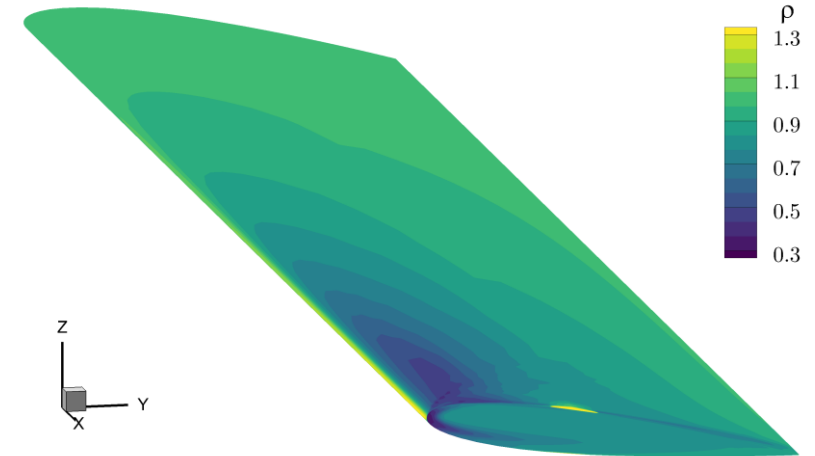
x2 EBR-WENO5



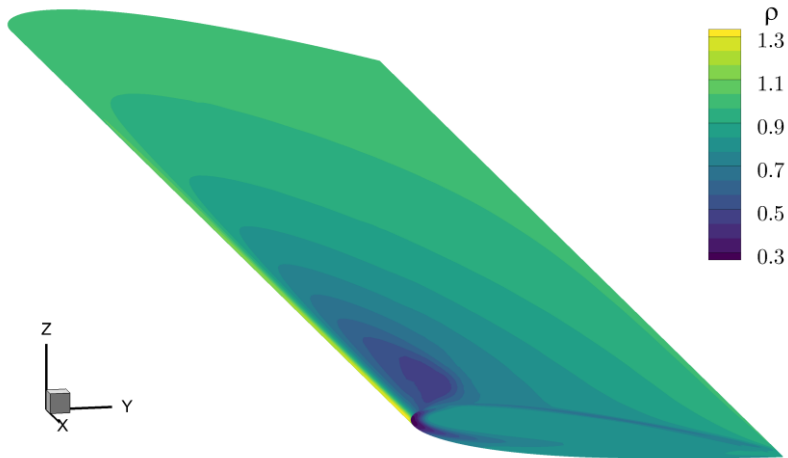
x1 EBR-WENO5



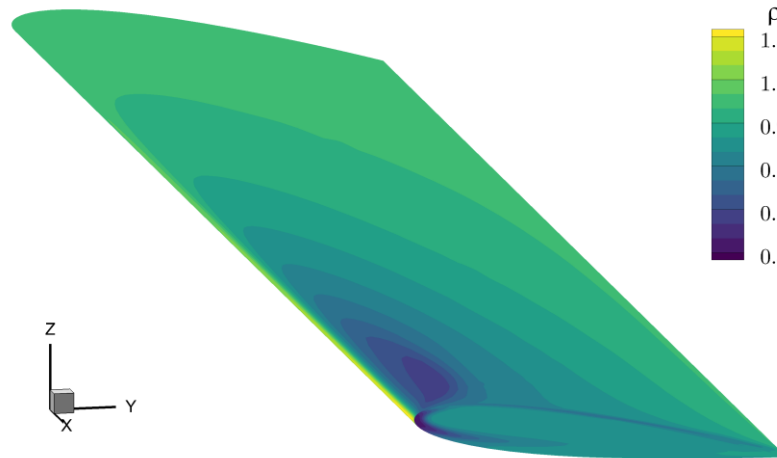
x1c EBR-WENO5



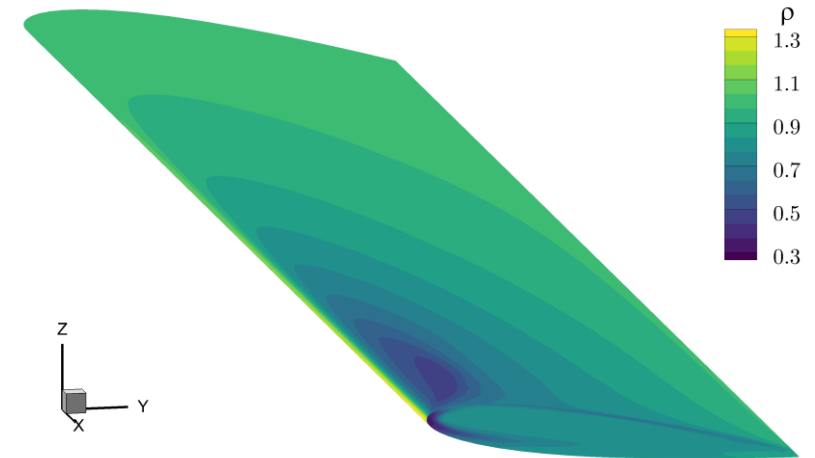
x2 EBR-WENO5 PL



x1 EBR-WENO5 PL



x1c EBR-WENO5 PL



- EBR IJK and EBR PL schemes proved to increase accuracy of numerical solution on coarse structured and prismatic meshes in comparison with the standard EBR scheme with straight-line reconstructions in boundary layer region
- EBR IJK and EBR PL schemes showed their possibility to increase accuracy in boundary layer even on fine meshes at least in density and friction coefficient distributions
- EBR IJK and EBR PL schemes demonstrated better stability qualities as expected

- More detailed description of the method and corresponding numerical results currently can be found in

Bakhvalov P., Duben A., Kozubskaya T., Rodionov P. Curvilinear Reconstructions for EBR Schemes On Semi-Structured Meshes. WCCM-ECCOMAS 2020 Paper. URL: https://www.scipedia.com/public/Bakhvalov_et_al_2021a